

1 **Intercomparison of bias correction methods for precipitation of** 2 **multiple GCMs across six continents**

3 Young Hoon Song¹, Eun-Sung Chung^{1*}

4 ¹ Faculty of Civil Engineering, Seoul National University of Science and Technology, 232 G
5 ongneung-ro, Nowon-gu, Seoul 01811, Korea

6
7 * Correspondence to: Eun-Sung Chung eschung@seoultech.ac.kr

8 9 **Abstract**

10 This study, conducted across six continents, evaluated and compared the effectiveness of three
11 Quantile Mapping (QM) methods: Quantile Delta Mapping (QDM), Empirical Quantile
12 Mapping (EQM), and Detrended Quantile Mapping (DQM) for correcting daily precipitation
13 data from 11 CMIP6 General Circulation Models (GCMs). The performance of corrected
14 precipitation data was evaluated using ten evaluation metrics, and the Technique for Order of
15 Preference by Similarity to Ideal Solution (TOPSIS) was applied to calculate performance-
16 based priorities. Bayesian Model Averaging (BMA) was used to quantify model-specific and
17 ensemble prediction uncertainties. Subsequently, this study developed a comprehensive index
18 by aggregating the performance scores from TOPSIS with the uncertainty metrics from BMA.
19 The results showed that EQM performed the best on all continents, effectively managing
20 performance and uncertainty. QDM outperformed other methods in specific regions and was
21 selected more frequently than DQM when greater weight was given to uncertainty. It suggests
22 that daily precipitation corrected by QDM is more stable than DQM. On the other hand, DQM
23 effectively reproduces dry climate but shows the highest uncertainty in certain regions,
24 suggesting potential limitations in capturing long-term climate trends. This study emphasizes
25 that both performance and uncertainty should be considered when choosing a bias correction
26 method to increase the reliability of climate predictions.

27 28 **Keywords**

29 CMIP6 GCM, Bias correction, Uncertainty, TOPSIS, Comprehensive index

31 **1. Introduction**

32 The Coupled Model Intercomparison Project (CMIP) General Circulation Models
33 (GCMs) have provided critical scientific evidence to explore climate change (IPCC, 2021;
34 IPCC, 2022). Nevertheless, GCMs exhibit significant biases compared to observational data
35 for reasons such as incomplete model parameterization and inadequate understanding of key
36 physical processes (Evin et al., 2024; Zhang et al., 2024; Nair et al., 2023). These deficiencies
37 with GCM have introduced various uncertainties in climate projections, making ensuring
38 sufficient reliability in climate change impact assessments difficult. In this context, many
39 studies have proposed various bias correction methods to reduce the discrepancies between
40 observational data and GCM simulations, thereby providing more stable results than raw GCM-
41 based assessments (Cannon et al., 2015; Themeßl et al., 2012; Piani et al., 2010). Despite these
42 advancements, the suggested bias correction methods differ in their physical approaches,
43 resulting in discrepancies in the climate variables adjusted for historical periods. Furthermore,
44 the distribution of precipitation across continents and specific locations causes variations in the
45 correction outcomes depending on the method used, which makes it challenging to reflect
46 extreme climate events in future projections and adds another layer of confusion to climate
47 change research (Song et al., 2022b; Maraëun, 2013; Ehret et al., 2012; Enayati et al., 2021).
48 Thus, exploring multiple aspects to make reasonable selections when applying bias correction
49 methods specific to each continent and region is necessary.

50 Many studies have developed appropriate bias correction methods based on various
51 theories, which have reduced the difference between GCM simulations and observed
52 precipitation (Abdelmoaty and Papalexiou, 2023; Shanmugam et al., 2024; Rahimi et al., 2021).
53 Quantile Mapping (QM) series has been widely adopted among bias correction methods due to
54 its conceptual simplicity, ease of application, and adaptability to various methodologies.
55 However, although common QM methods have high performance in correcting stationary
56 precipitation, they are less efficient in non-stationary data, such as extreme precipitation events
57 (Song et al., 2022b). To address these limitations, a recent study proposed an improved QM
58 approach to reflect future non-stationary precipitation across all quantiles of historical
59 precipitation (Rajulapati and Papalexiou, 2023, Cannon et al., 2015, Cannon, 2018; Song et al.,
60 2022b). In recent years, climate studies using GCMs have adopted several improved QM
61 methods that offer higher performance than previous methods to correct historical precipitation
62 and project it accurately into the future. For example, Song et al. (2022b) performed bias

63 correction on daily historical precipitation over South Korea using distribution transformation
64 methods they developed and found that the best QM method varied depending on the station.
65 Additionally, previous studies have reported that QM performance varied by grid and station
66 (Ishizaki et al., 2022; Chua et al., 2022). From this perspective, these improved QMs may only
67 guarantee uniform results across some grids and regions. Therefore, to analyze positive
68 changes in future climate impact assessments, it is essential to select appropriate bias correction
69 methods based on a robust framework.

70 Multi-criteria decision analysis (MCDA) is efficient for prioritization because it can
71 aggregate diverse information from various alternatives. MCDA has been extensively used
72 across different fields to select suitable alternatives, with numerous studies confirming its
73 stability in priority selection (Chae et al., 2022; Chung and Kim, 2014; Song et al., 2024).
74 Moreover, MCDA has been employed in future climate change studies to provide reasonable
75 solutions to emerging problems, including the selection of bias correction methods for specific
76 regions and countries (Homsy et al., 2019; Saranya and Vinish, 2021). However, MCDA's
77 effectiveness is sensitive to the source and quality of alternatives, making accurate ranking
78 challenging when information is lacking or overly focused on specific criteria (Song and Chung,
79 2016). Small-scale regional and observation-based studies have conducted GCM performance
80 evaluations, but global and continental-scale evaluations are rare due to the substantial time
81 and cost required.

82 GCM simulation includes uncertainties from various sources, such as model structure,
83 initial condition, boundary condition, and parameters (Pathak et al., 2023; Cox and Stephenson,
84 2007; Yip et al., 2011; Woldemeskel et al., 2014). The selection of bias correction methods
85 contributes significantly to uncertainty in climate change research using GCMs. Jobst et al.
86 (2018) argued that GHG emission scenarios, bias correction methods, and GCMs are primary
87 sources of uncertainty in climate change assessments across various fields. The extensive
88 uncertainties in GCMs complicate the efficient establishment of adaptation and mitigation
89 policies. This issue has led to the increased awareness of the uncertainties inherent in historical
90 simulations. Consequently, many studies have focused on estimating uncertainties using
91 diverse methods to quantify these uncertainties (Giorgi and Mearns, 2002; Song et al., 2022a,
92 Song et al., 2023). Although it is impossible to drastically reduce the uncertainty of GCM
93 outputs due to the unpredictable nature of climate phenomena, uncertainties in GCM
94 simulations can be reduced using ensemble principles, such as multi-model ensemble

95 development using rational approach (Song et al., 2024). However, accurately identifying
96 biases in simulation precipitation remains challenging due to the lack of comprehensive
97 equations reflecting Earth's physical processes. In this context, climate change studies have
98 aimed to quantify the uncertainty of historical climate variables in GCMs, offering insights into
99 the variability of GCM simulations (Pathak et al., 2023). Bias-corrected precipitation of GCMs
100 using QM has shown high performance in the historical period, which is expected to result in
101 better future predictions. However, the physical concepts of various QMs may lead to more
102 significant uncertainty in the future (Lafferty et al., 2023). Therefore, efforts should be made
103 to consider and reduce uncertainty in the GCM selection process. It will ensure the reliability
104 of predictions by selecting an appropriate bias-correcting method.

105 This study aims to compare the performance of three bias correction methods using
106 daily historical precipitation data (1980-2014) from CMIP6 GCMs across six continents (South
107 America: SA; North America: NA; Africa: AF; Europe: EU; Asia: AS; and Oceania: OA). Ten
108 evaluation metrics were used to assess the performance of daily precipitation corrected by the
109 three QM methods for each continent. Subsequently, the Technique for Order of Preference by
110 Similarity to Ideal Solution (TOPSIS) of MCDA was applied to select an appropriate bias
111 correction method for each continent. Additionally, the uncertainty in daily precipitation for
112 historical periods was quantified using Bayesian Model Averaging (BMA). By integrating
113 performance scores from TOPSIS and uncertainty metrics from BMA, this study developed a
114 Comprehensive Index (CI), which was then used to select the best bias correction method for
115 each continent. This comprehensive approach ensures a balanced consideration of both
116 performance and uncertainty, enhancing understanding of the bias correction process based on
117 the distribution of daily precipitation across continents.

118

119 **2. Datasets and methods**

120 **2.1 General Circulation Model**

121 This study used 11 CMIP6 GCM to perform bias correction for daily precipitation in the
122 historical period. Only daily precipitation was used in performing bias correction in this study
123 because the natural variability relative to projected anthropogenically forced trends is much
124 larger for precipitation than for temperature (Deser et al., 2012). Table 1 presents the basic
125 information, such as model names, resolution, and variant labels. The model resolution of 11

126 CMIP6 GCMs was equally re-gridded to $1^\circ \times 1^\circ$ using linear interpolation. Furthermore, this
 127 study's ensemble member of CMIP6 GCMs was the first member of realizations (r1).

128

129 Table 1. Information of CMIP6 GCMs in this study

Models	Resolution	Climate variables	Variant label
ACCESS-CM2	$1.2^\circ \times 1.8^\circ$	Daily precipitation	r1i1p1f1
ACCESS-ESM1-5	$1.2^\circ \times 1.8^\circ$		
BCC-CSM2-MR	$1.1^\circ \times 1.1^\circ$		
CanESM5	$2.8^\circ \times 2.8^\circ$		
CESM2-WACCM	$0.9^\circ \times 1.3^\circ$		
CMCC-CM2-SR5	$\sim 0.9^\circ$		
CMCC-ESM2	$0.9^\circ \times 1.25^\circ$		
EC-Earth3-Veg-LR	$1.0^\circ \times 1.0^\circ$		
GFDL-ESM4	$1.4^\circ \times 1.4^\circ$		
INM-CM4-8	$\sim 0.9^\circ$		
IPSL-CM6A-LR	$1.1^\circ \times 1.1^\circ$		

130

131 2.2 Reference data

132 This study utilized ERA5 reanalysis data from the European Center for Medium-Range
 133 Weather Forecasts (ECMWF) as reference data. The model physics of ERA5 reanalysis data
 134 improved as it employed an Integrated Forecasting System based on CY41r2 (Hersbach et al.,
 135 2020). The model resolution selected in this study was $1.0^\circ \times 1.0^\circ$, which was provided by the
 136 institution for research availability. The accuracy of assessing GCM simulation is crucial for
 137 replicating the spatial and temporal variability of observed data (Hamed et al., 2023). In this
 138 context, the ERA5 product has been commonly used to reproduce observed precipitation, for
 139 the evaluation of GCMs' performances.

140

141 2.3 Quantile mapping

142 This study employed three (Quantile delta mapping, QDM; Detrended quantile mapping, DQM;
 143 Empirical quantile mapping, EQM) QM methods to correct the simulation of CMIP6 GCMs,
 144 and these methods are commonly used in the climate change research based on the climate
 145 models (Switanek et al., 2017). This study divided the data into a training period (1980-1996)
 146 and a validation period (1997-2014) to correct the historical period's data. Furthermore, the
 147 historical precipitation corrected using the three QM methods was compared for performance
 148 against reference data across six continents. The frequency-adaptation technique, as described
 149 by Themeßl et al. (2012), was applied to address potential biases and improve the accuracy of

150 the corrections. The corrected precipitation using the QM used a cumulative distribution
 151 function, as shown in Equation 1, to reduce the difference from the reference data.

$$152 \hat{x}_{m,p}(t) = F_{o,h}^{-1}\{F_{m,h}[x_{m,p}(t)]\} \quad (1)$$

153 where, $\hat{x}_{m,p}(t)$ presents the bias-corrected results. $F_{o,h}$ represents the cumulative distribution
 154 function (CDF) of the observed data, and $F_{m,h}$ presents the CDF of the model data. The
 155 subscripts o and m denote observed and model data, respectively, and the subscript h denotes
 156 the historical period.

157 QDM, developed by Cannon et al. (2015), preserves the relative changes ratio of modeled
 158 precipitation quantiles. In this context, QDM consists of bias correction terms derived from
 159 observed data and relative change terms obtained from the model. The computation process of
 160 QDM is carried out as described in Equation (2) to (4).

$$161 \hat{x}_{m,p}(t) = \hat{x}_{o:m,h;p}(t) \cdot \Delta_m(t) \quad (2)$$

$$162 \hat{x}_{o:m,h;p}(t) = F_{o,h}^{-1}\{F_{m,p}^{(t)}[x_{m,p}(t)]\} \quad (3)$$

$$163 \Delta_m(t) = \frac{x_{m,p}(t)}{F_{m,h}^{-1}\{F_{m,p}^{(t)}[x_{m,p}(t)]\}} \quad (4)$$

164 where, $\hat{x}_{o:m,h;p}(t)$ presents the bias corrected daily precipitation for the historical period, and
 165 $\Delta_m(t)$ the relative change in the model simulation between the reference period and the target
 166 period. In addition, the target period is calculated by multiplying the relative change ($\Delta_m(t)$)
 167 at time (t) multiplied by the bias-corrected precipitation in the reference period. $\Delta_m(t)$ is
 168 defined as $\widehat{\bar{x}_{m,p}}(t)$ divided by $F_{o,h}^{-1}\{F_{m,p}^{(t)}[x_{m,p}(t)]\}$. $\Delta_m(t)$ preserving the relative change
 169 between the reference and target periods. DQM, while more limited compared to QDM,
 170 integrates additional information regarding the projection of future precipitation. Furthermore,
 171 climate change signals estimated from DQM tend to be consistent with signals from baseline
 172 climate models. The computational process of DQM is performed as shown in Equation (5).

$$173 \hat{x}_{m,p} = F_{o,h}^{-1}\left\{F_{m,h}\left[\frac{\bar{X}_{m,h}X_{m,h}(t)}{\bar{X}_{m,p}(t)}\right]\right\} \frac{\bar{X}_{m,p}(t)}{\bar{X}_{m,h}} \quad (5)$$

174 where, $\bar{X}_{m,h}$ and $\bar{X}_{m,p}$ represent the long-term modeled averages for the historical reference
 175 period and the target period, respectively.

176 EQM is a method that corrects the quantiles of the empirical cumulative distribution function
 177 from a GCM simulation based on a reference precipitation distribution using a corrected
 178 transfer function (Dequé, 2007). The calculation process of EQM can be represented as follows
 179 in Equation (6).

180 $\hat{x}_{m,p}(t) = F_{o,h}^{-1}(F_{m,h}(x_{m,p}(t)))$ (6)

181 All these QMs can be applied to the historical data correction in this approach. The bias
 182 correction is performed based on the relative changes between a reference period and a target
 183 period in the past, ensuring that the relative changes between these periods are preserved in the
 184 corrected data (Ansari et al., 2023; Tanimu et al., 2024; Cannon et al., 2015).

185

186 **2.4 Evaluation metrics**

187 This study used the ten-evaluation metrics to assess the output performance of three quantile
 188 mapping methods against the reference data for the validation period (1997-2014). Seven
 189 evaluation metrics used in this study are as follows: Root Mean Square Error (RMSE), Mean
 190 Absolute Error (MAE), Coefficient of Determination (R^2), Percent bias (Pbias), Nash-Sutcliffe
 191 Efficiency (NSE), Kling-Gupta efficiency (KGE), Median Absolute Error (MdAE), Mean
 192 Squared Logarithmic Error (MSLE), Explained Variance Score (EVS), and Jensen-Shannon
 193 divergence (JS-D). The equations of seven evaluation metrics are presented in Table 2.

194

195 Table 2. Information of the seven-evaluation metrics used in this study

Metrics	Equations	Factors	References
RMSE	$= \sqrt{\frac{1}{n} \sum_{i=1}^n (X_i^{sim} - X_i^{ref})^2}$	X_i^{ref} reference data X_i^{sim} Bias corrected GCM	
MAE	$= \sum_{i=1}^n X_i^{sim} - X_i^{ref} $		
R^2	$= 1 - \frac{\sum_{i=1}^n (X_i^{sim} - X_i^{ref})^2}{(\sum_{i=1}^n X_i^{ref} - \bar{X}_i^{ref})^2}$		Galton, 1886
Pbias	$= \frac{\sum_{i=1}^n (X_i^{ref} - X_i^{sim})}{\sum_{i=1}^n X_i^{ref}} \times 100$		
NSE	$= 1 - \frac{\sum_{i=1}^n (X_i^{sim} - X_i^{ref})^2}{\sum_{i=1}^n (X_i^{ref} - \bar{X}_i^{ref})^2}$		Nash and Sutcliffe, 1970
MdAE	$= median(X_i^{sim} - X_i^{ref})$		

MSLE	$= \frac{1}{n} \sum_{i=1}^n (\log(1 + X_i^{sim}) - \log(1 + X_i^{ref}))^2$		
EVS	$= 1 - \frac{Var(X^{sim} - X^{ref})}{Var(X^{ref})}$		
KGE	$= 1 - \sqrt{(r - 1)^2 + (\alpha - 1)^2 + (\beta - 1)^2}$	r Pearson product-moment correlation α Variability error β : Bias term	Gupta et al. 2009
JS-D	$= \frac{1}{2} D_{KL} \left(P \parallel \frac{P + Q}{2} \right) + \frac{1}{2} D_{KL} \left(Q \parallel \frac{P + Q}{2} \right)$	$P(x)$: Probability density distribution of reference data $Q(x)$: Probability density distribution of GCM D_{KL} : KL-D	Lin, 1991

196

197 Ten-evaluation metrics selected in this study assess GCM performance from various
198 perspectives, including error (RMSE, MAE, MdAE, and MSLE), deviation (Pbias), accuracy (
199 R^2 , NSE), variability (EVS), correlation and overall performance (KGE), and distributional
200 differences (JSD). These metrics complement each other by offering a comprehensive
201 evaluation framework. For instance, while NSE evaluates the overall fit of the simulated data
202 to observations, KGE provides a holistic view by integrating correlation, variability, and bias
203 into a single efficiency score, and JS-D captures the difference between the distributions of the
204 reference data and the bias-corrected GCM output.

205

206 **2.5 Generalized extreme value**

207 This study used generalized extreme value (GEV) to compare the extreme precipitation
208 calculated by the bias-corrected GCM at each grid of six continents over the historical period.
209 The historical precipitation was compared with the distribution of reference data and bias-
210 corrected GCM above the 95th quantile of the Probability Density Function (PDF) of the GEV
211 distribution (Hosking et al. 1985). In addition, this study compared the distribution differences

212 between the reference data based on the GEV distribution and the corrected GCM using JSD.
 213 GEV distribution is commonly used to confirm extreme values in climate variables. The PDF
 214 of the GEV distribution is shown in Equation 7, and the parameters of the GEV distribution
 215 were estimated using L-moment (Hosking, 1990).

$$216 \quad g(x) = \frac{1}{\alpha} \left[1 - k \frac{x-\epsilon}{\alpha} \right]^{\frac{1}{k}-1} \exp \left\{ - \left[1 - k \frac{x-\epsilon}{\alpha} \right]^{\frac{1}{k}} \right\} \quad (7)$$

217 where, k , α , and ϵ represents a shape, scale, and location of the GEV distribution, respectively.
 218

219 **2.6 Bayesian model averaging (BMA)**

220 The BMA is a statistical technique that combines multiple models to provide predictions that
 221 account for model uncertainty (Hoeting et al., 1999). BMA is used to integrate predictions from
 222 GCMs to improve the robustness and reliability of the resulting assemblies. The posterior
 223 probability of each model is calculated based on Bayes' theorem as shown in Equation 8.

$$224 \quad P(M_k | D) = \frac{P(D|M_k)P(M_k)}{\sum_{j=1}^K P(D|M_j)P(M_j)} \quad (8)$$

225 where, $P(M_k)$ is the prior probability of model M_k , and $P(D | M_k)$ is the likelihood of the data
 226 D given model M_k , $P(M_k | D)$ is the posterior probability of model M_k . In addition, the BMA
 227 prediction \hat{Q}_{BMA} is the weighted average of the predictions from each model as shown in
 228 Equation 9.

$$229 \quad \hat{Q}_{BMA} = \sum_{k=1}^K P(M_k | D) \hat{Q}_k \quad (9)$$

230 where, \hat{Q}_k is the prediction from model M_k . In this study, BMA was used to quantify the model
 231 uncertainty and ensemble prediction uncertainty for daily precipitation corrected by three QM
 232 methods (QDM, EQM, and DQM) applied to 11 CMIP6 GCMs, as shown in Equations 10 and
 233 11.

$$234 \quad \alpha_w^2 = \frac{1}{K} \sum_{k=1}^K (w_k - \bar{w})^2 \quad (10)$$

235 where, K is the number of models, $w_k = P(M_k | D)$ is the weight of model M_k , \bar{w} is the mean
 236 of the weights, given by $\bar{w} = \frac{1}{K} \sum_{k=1}^K w_k$. A higher variance in model weights indicates more
 237 significant prediction differences, implying greater model uncertainty.

$$238 \quad \sigma_{BMA} = \sqrt{\frac{1}{K} \sum_{k=1}^K (\hat{Q}_k - \hat{Q}_{BMA})^2} \quad (11)$$

239 σ_{BMA} is standard deviation of the BMA ensemble predictions, \hat{Q}_k is the prediction from each
 240 model M_k , \hat{Q}_{BMA} is the weighted average prediction from BMA. This standard deviation

241 represents the variability among the ensemble predictions and serves as an indicator of
 242 uncertainty. A lower standard deviation implies higher consistency among predictions,
 243 indicating lower uncertainty, while a higher standard deviation suggests greater variability and
 244 higher uncertainty.

245

246 **2.7 TOPSIS**

247 This study used TOPSIS to calculate a rational priority among three QM methods based on the
 248 outcomes derived from evaluation metrics. Furthermore, the closeness coefficient calculated
 249 using TOPSIS was used as the performance metric for the CI. Proposed by Hwang and Yoon
 250 (1981), TOPSIS is a multi-criteria decision-making technique frequently used in water
 251 resources and climate change research to select alternatives (Song et al., 2024). As described
 252 in Equation 12 and 13, the proximity of the three QM methods is calculated based on the
 253 Positive Ideal Solution (PIS) and the Negative Ideal Solution (NIS).

$$254 \quad D_i^+ = \sqrt{\sum_{j=1}^n w_j (f_j^+ - f_{i,j})^2} \quad (12)$$

$$255 \quad D_i^- = \sqrt{\sum_{j=1}^n w_j (f_j^- - f_{i,j})^2} \quad (13)$$

256 where, D_i^+ is the Euclidean distance of each criterion from the PIS, summing the whole criteria
 257 for an alternative f_j^+ , j presents the normalized value for the alternative f_j^+ . w_j presents weight
 258 assigned to the criterion j . D_i^- is the distance between the alternative f_j^- and the NIS. The
 259 relative closeness is calculated as shown in Equation 14. The optimal value is closer to 1 and
 260 represents a reasonable alternative.

$$261 \quad C_i = \frac{D_i^-}{(D_i^- + D_i^+)} \quad (14)$$

262

263 **2.8 Comprehensive index (CI)**

264 This study proposed a CI to select the best QM method by combining performance scores and
 265 model uncertainty indicators. The CI integrates the performance scores (closeness coefficient)
 266 derived from the TOPSIS method with the uncertainty quantified using BMA. This approach
 267 allows for a balanced evaluation that considers both the effectiveness of the QM methods and
 268 the associated uncertainties. Uncertainty was quantified in two ways. Model-specific weight
 269 variance was calculated using the variance of the model weights assigned by BMA,
 270 representing the uncertainty in selecting the appropriate QM. The standard deviation of BMA

271 ensemble prediction was calculated to capture the spread and, thus, the uncertainty of the
272 ensemble forecasts. Both the indicators were normalized using min-max scaler to ensure
273 comparability. Finally, the calculation process of the CI is performed as shown in Equations
274 15 and 16.

$$275 \quad UI = \frac{V_w + \sigma_e}{2} \quad (15)$$

$$276 \quad CI = \alpha \times C_i - \beta \times UI \quad (16)$$

277 where, UI represents the uncertainty indicator. V_w and σ_e represent the normalized weight
278 variance and the normalized ensemble standard deviation, respectively, calculated using BMA.
279 C_i represents the closeness coefficient calculated from TOPSIS. α represents the weight given
280 to the performance score, β represents the weight given to the uncertainty indicator.
281 Furthermore, by adjusting the weights α and β , the study evaluated the QM methods under
282 different scenarios. Equal weight ($\alpha = 0.5, \beta = 0.5$) balances performance and uncertainty
283 equally, and the emphasized performance weight ($\alpha = 0.7, \beta = 0.3$) prioritize performance over
284 uncertainty. The emphasized uncertainty weight ($\alpha = 0.3, \beta = 0.7$) prioritize uncertainty over
285 performance. The results from the CI provide a holistic evaluation of the QM methods,
286 considering both their effectiveness in bias correction and the reliability of their predictions.

287

288 **3. Result**

289 **3.1 Assessment of bias correction reproducibility across continents**

290 **3.1.1 Comparison of bias correction effects**

291 This study applied three QM methods to correct daily precipitation data from 11 CMIP6 GCMs
292 across six continents. Figure 1 presents the results of comparing daily precipitation data before
293 and after bias correction using Taylor diagram. In general, the precipitation corrected by DQM
294 showed a larger difference from the reference data than other methods. In contrast, EQM
295 showed better performance overall than DQM, and many models showed results that were
296 close to the reference data. The precipitation corrected by QDM also showed good performance
297 in most continents but slightly lower than EQM. Nevertheless, QDM showed clearly better
298 results than DQM.

299 In terms of correlation coefficients, precipitation corrected by DQM showed relatively high
300 values between 0.8 and 0.9 but lower than EQM and QDM. The precipitation corrected by
301 EQM showed high agreement with the reference data, recording correlation coefficients above

302 0.9 in most continents. QDM generally showed similar correlation coefficients to EQM but
303 slightly lower values than EQM in North America and Asia.

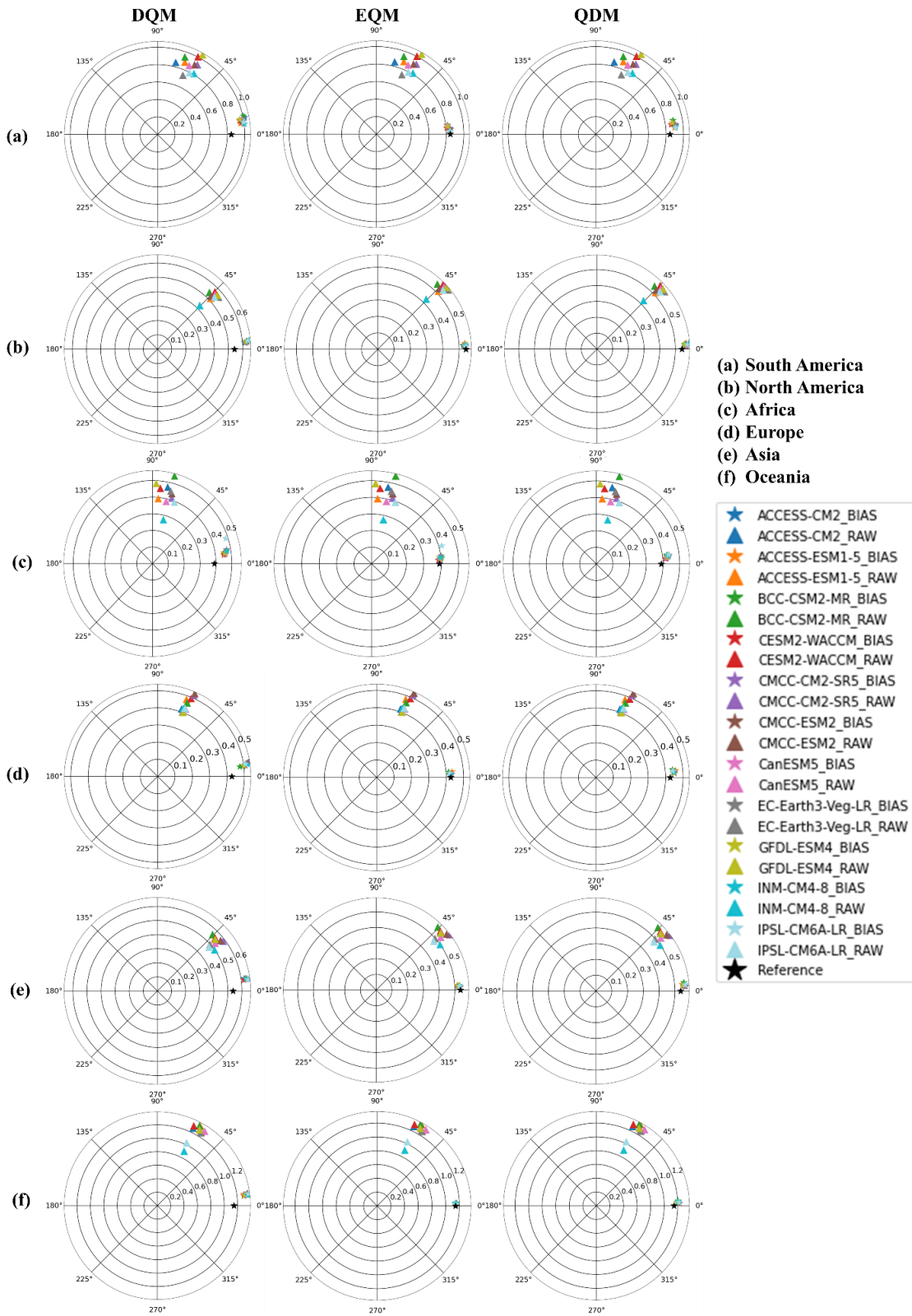
304 For RMSE, precipitation corrected by DQM was higher than EQM and QDM, indicating that
305 the corrected precipitation differed more from the reference data. On the other hand, EQM had
306 the lowest RMSE and showed superior performance compared to other methods. QDM had
307 slightly higher RMSE than EQM but still outperformed DQM.

308 In terms of standard deviation, precipitation corrected by DQM was higher or lower than the
309 reference data in most continents. On the other hand, precipitation corrected by EQM was
310 similar to the reference data and almost identical to the reference data in Africa and Asia. QDM
311 was similar to the reference data in some continents but showed slight differences from EQM.

312 These results imply that the precipitation corrected by the three methods outperforms the raw
313 simulation, which confirms that the GCM's daily precipitation is reliably corrected in the
314 historical period.

315

Taylor diagram



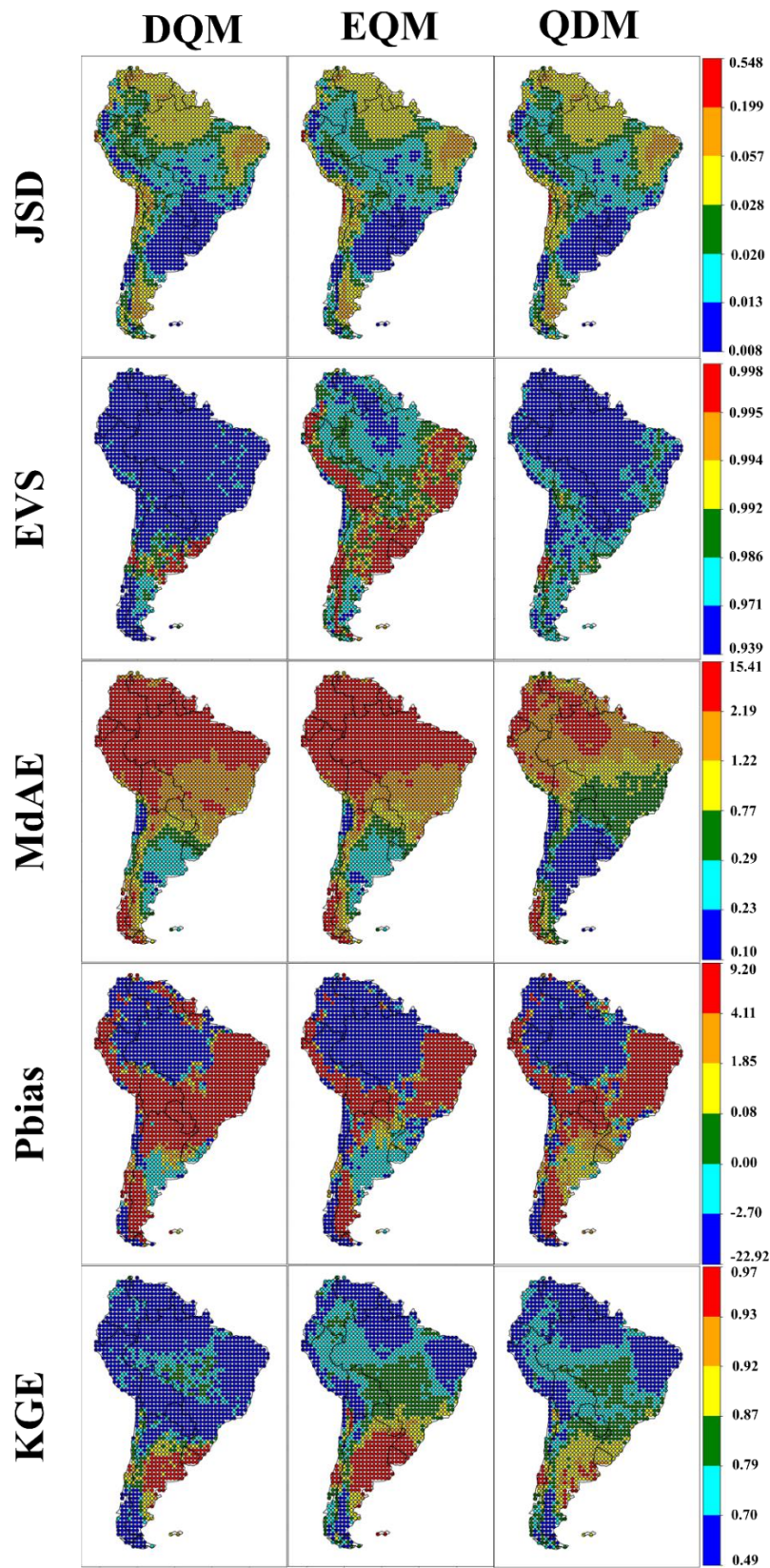
316

317 Figure 1. Comparison of raw and corrected daily precipitation on six continents using Taylor

318 diagrams

319 **3.1.2 Spatial distribution of bias correction performance**

320 This study evaluated the performance of daily precipitation across six continents using ten
321 evaluation metrics for 11 CMIP6 GCMs. Figures 2 and S1 present the spatial patterns of these
322 evaluation metrics, calculated for daily precipitation from the bias corrected GCMs in South
323 America. Overall, the precipitation corrected by EQM demonstrated lower JSD values, as well
324 as higher EVS and KGE values, compared to other methods. The precipitation corrected by
325 EQM showed higher EVS in certain regions but slightly lower performance in MDAE and Pbias
326 across some grids. DQM exhibited performance similar to EQM and QDM in most evaluation
327 indices but was relatively lower in most evaluation metrics. The precipitation corrected by the
328 three methods was underestimated compared to the reference data in northern South America,
329 while it was overestimated in eastern South America. In addition, precipitation corrected by
330 the DQM method tended to be overestimated more than the other methods, while the EQM
331 method showed the opposite result. Furthermore, the daily precipitation corrected by EQM
332 showed the lowest overall error and high performance in both NSE and R^2 . QDM and DQM
333 also performed well but exhibited slightly larger errors in some regions than EQM.
334



335

336 Figure 2. Performance comparison of DQM, EQM, and QDM using evaluation metrics (JSD,

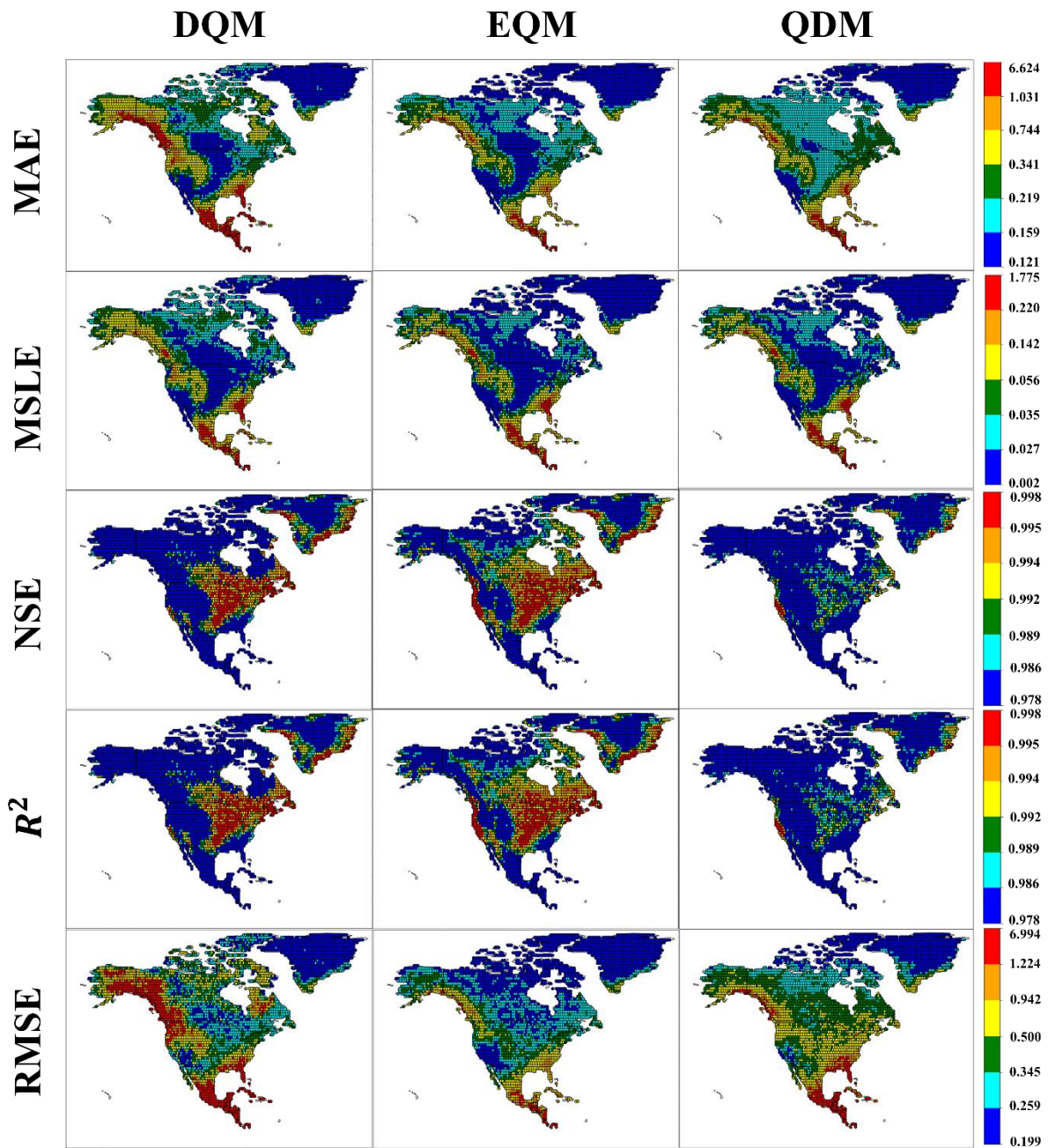
337 EVS, MdAE, Pbias, and KGE) for daily precipitation in South America.

338 Figures 3 and S2 present the spatial patterns of these evaluation metrics, calculated for daily
339 precipitation from the bias corrected GCMs in South America. Regarding error metrics (MAE,
340 MSLE, RMSE, and MdAE), precipitation corrected using DQM showed relatively lower
341 performance across North America, with particularly large errors in the southern region. In
342 contrast, precipitation corrected using EQM demonstrated superior performance across the
343 continent compared to other methods. QDM exhibited similar error performance to EQM but
344 slightly higher errors in the southern region.

345 For correlation metrics (NSE and R^2), DQM-corrected precipitation had lower performance
346 compared to other methods, although there were some grid cells in the central and eastern
347 regions that exhibited high performance, with values exceeding 0.995. The precipitation
348 corrected using EQM showed the highest performance, especially in the central and eastern
349 regions, where most grid points showed correlation coefficients as above 0.995. QDM, while
350 achieving correlation metrics above 0.978 for most grid points, had slightly lower performance
351 compared to the other methods.

352 Regarding Pbias, all three methods tended to overestimate precipitation relative to the reference
353 data across most grid points in North America, while corrected precipitation in Greenland was
354 underestimated. For JSD, EVS, and KGE metrics, EQM-corrected precipitation showed the
355 highest performance, with DQM and QDM performing lower than EQM.

356



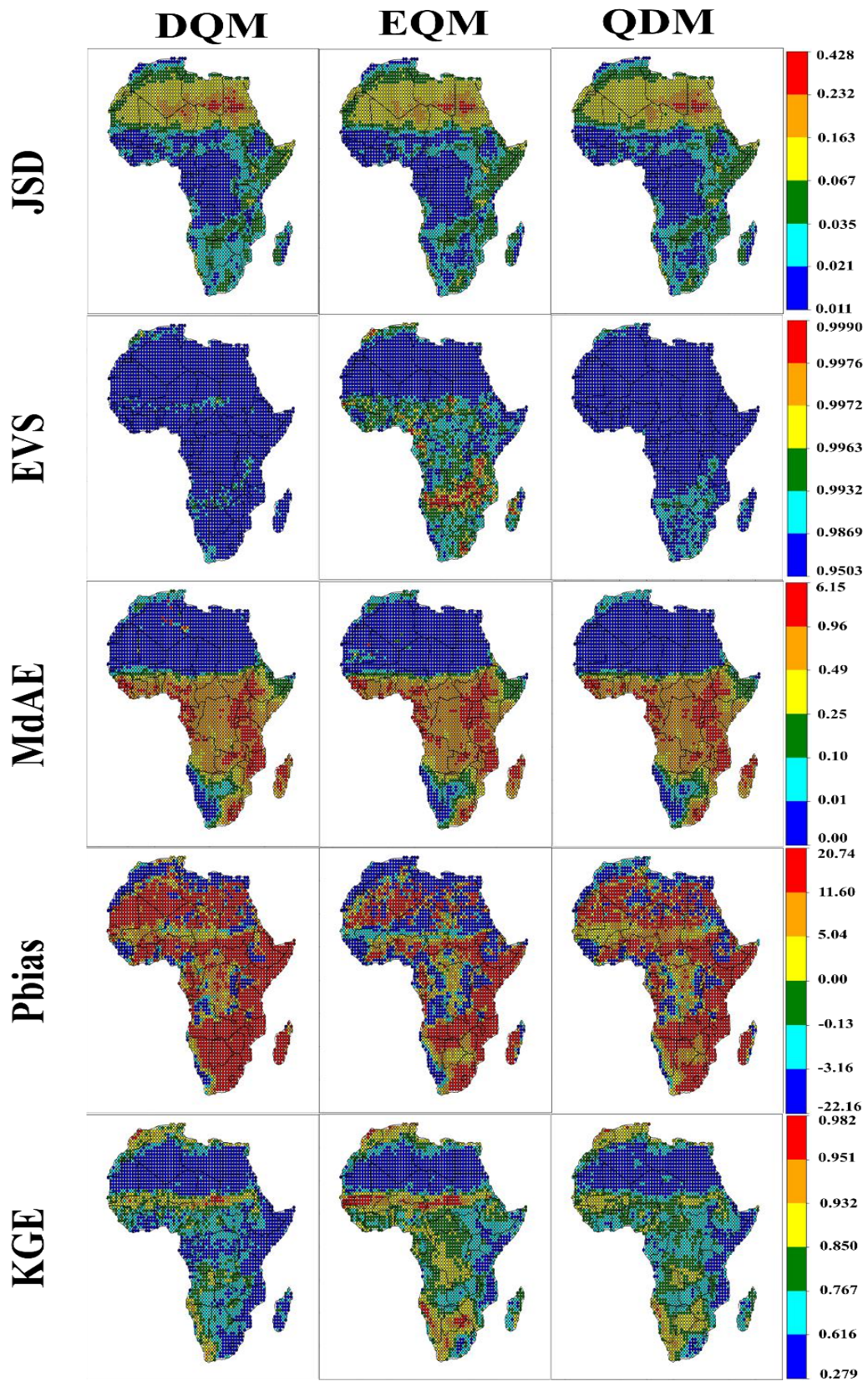
357

358 Figure 3. Performance comparison of DQM, EQM, and QDM using evaluation metrics (MAE,
 359 MSLE, NSE, R^2 , and RMSE) for daily precipitation in North America.

360

361 In this study, the daily precipitation in Africa was corrected using three QM methods, and the
 362 performance is shown in Figures 4 and S3. Overall, the JSD of precipitation corrected by the
 363 three methods showed similar spatial patterns, but the precipitation of DQM showed lower
 364 performance than the other methods in the southern region. In terms of EVS, the precipitation
 365 of DQM showed higher variability than the other methods. The precipitation of QDM showed

366 lower variability in southern Africa than DQM, but overall, it showed higher variability than
367 EQM. The precipitation of EQM showed lower variability in southern and central Africa but
368 still showed high variability in the northern region. Analyzing the error performance, the
369 precipitation corrected by QDM showed the best performance compared to the other methods.
370 In particular, QDM showed the highest performance in North Africa (MAE: 0.03, and MSLE:
371 0.004), and EQM's error performance was lower than QDM's in most indicators but better than
372 DQM's. Finally, EQM performed the highest in correlation metrics (NSE and R^2), and QDM
373 performed better than DQM.

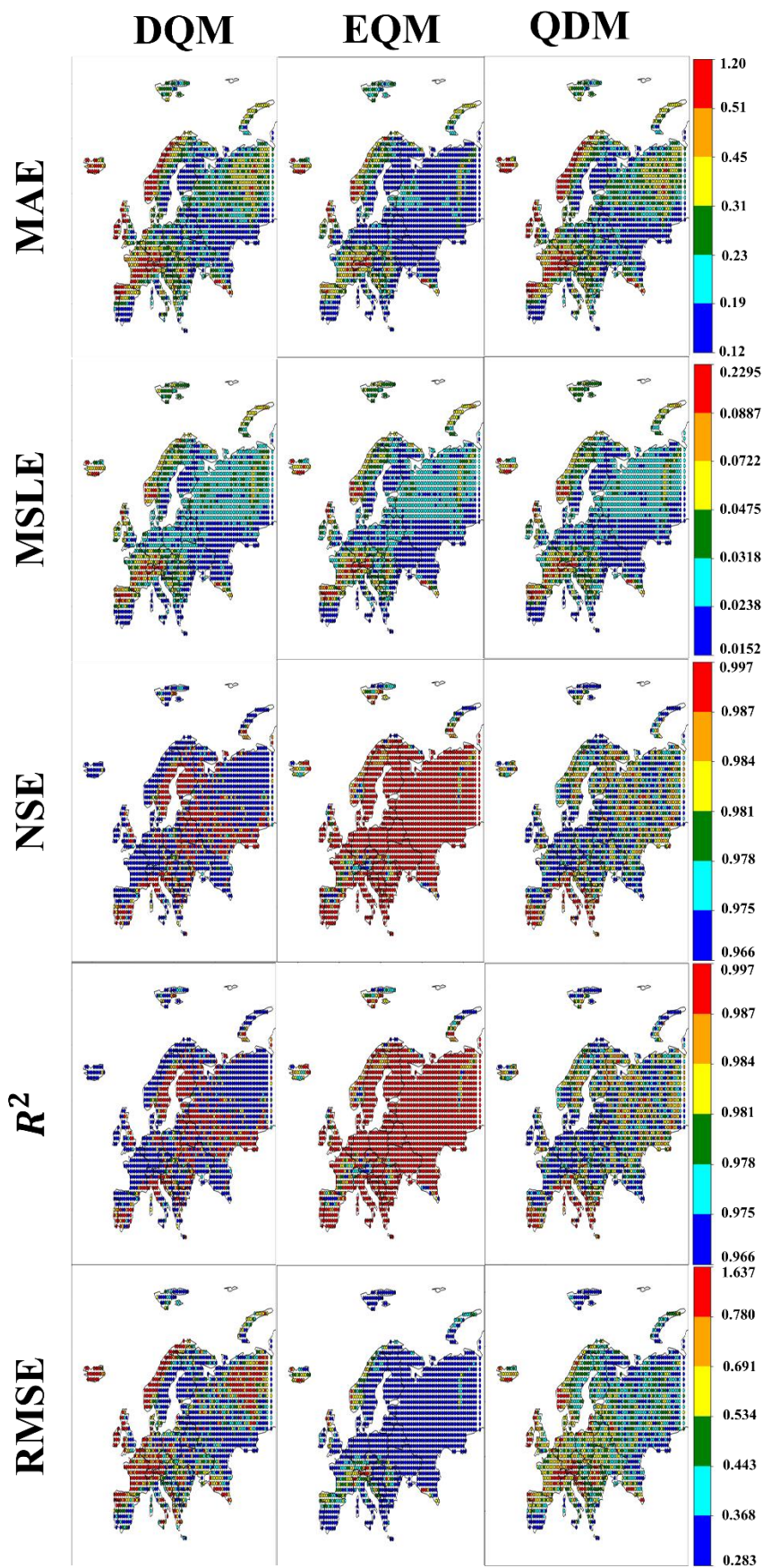


374

375 Figure 4. Performances of DQM, EQM, and QDM using evaluation metrics (JSD, EVS, MdAE,

376 Pbias, and KGE) for daily precipitation in Africa.

377 Figures 5 and S4 show the spatial results of the grid-based evaluation metrics for the European
378 region. In terms of error metrics, EQM-corrected precipitation performed the best across
379 Europe compared to other methods. In contrast, QDM-corrected precipitation performed
380 similarly to DQM in MAE and MSLE but significantly outperformed DQM in RMSE.
381 Regarding NSE and R, EVS, and KGE metrics, EQM-corrected precipitation performed
382 overwhelmingly better than other methods. QDM precipitation performed better than DQM,
383 while DQM performed the worst. Regarding Pbias, EQM-corrected precipitation was
384 underestimated compared to the reference data in most parts of Europe. In contrast, QDM-
385 corrected precipitation was more similar to the reference data compared to other methods, and
386 DQM precipitation was overestimated compared to the reference data except in central Europe.

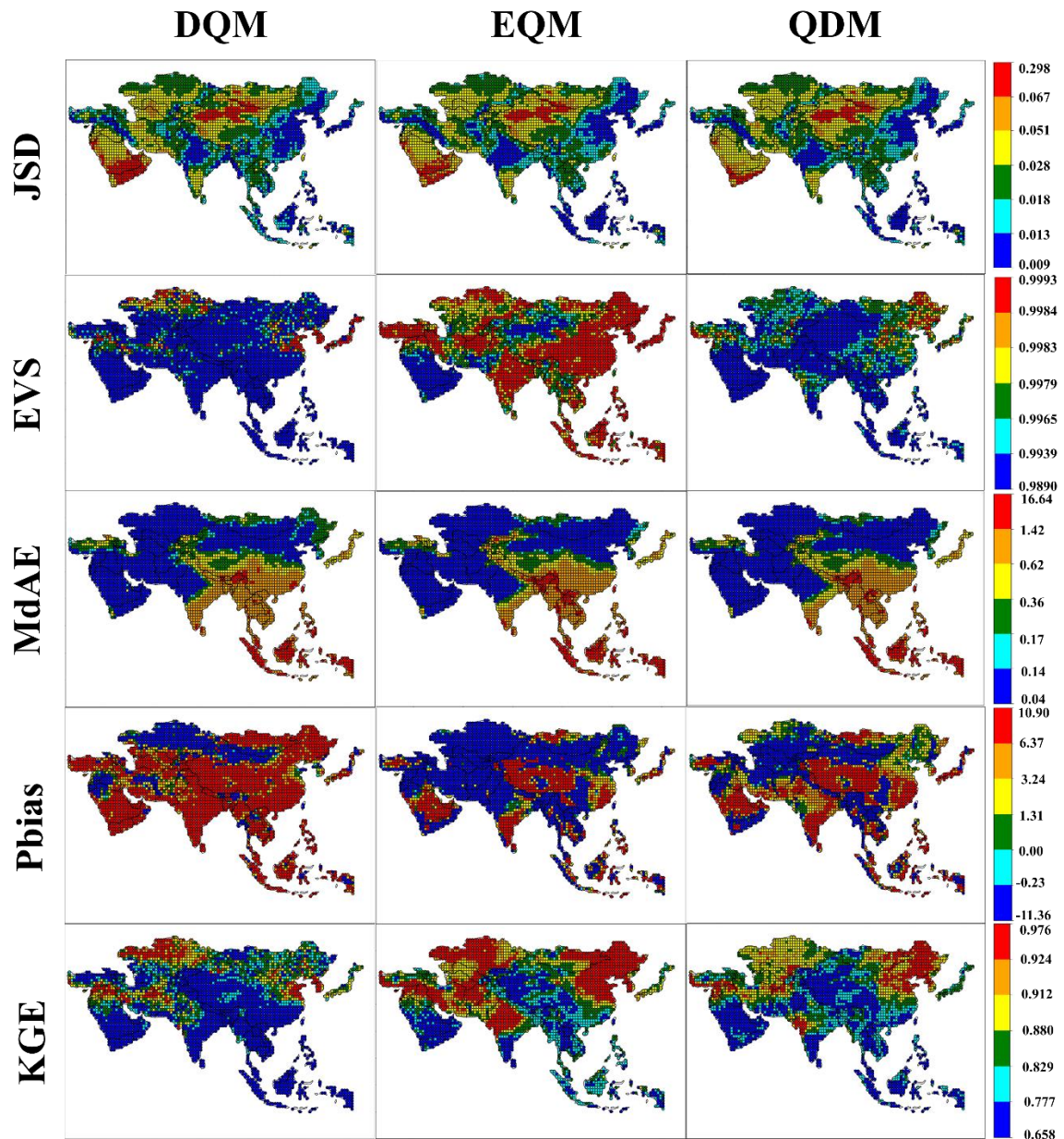


388 Figure 5. Performances of DQM, EQM, and QDM using evaluation metrics (MAE, MSLE,
389 NSE, R^2 , and RMSE) for daily precipitation in Europe.

390 Figures 6 and S5 show the results of spatially quantifying the corrected precipitation in Asia
391 using various evaluation metrics. When it comes to error metrics, EQM-corrected precipitation
392 stands out with its superior performance, particularly in RMSE, which was consistently below
393 1.35 in most areas of Asia, except for certain parts of Central Asia. In contrast, DQM-corrected
394 precipitation showed the poorest performance in error metrics. QDM-corrected precipitation
395 demonstrated a performance similar to EQM, but with a slightly lower performance in East
396 Asia and North Asia. In NSE and R, the precipitation corrected by EQM performed better than
397 other methods, especially in Southwest Asia and East Asia. In contrast, the precipitation
398 corrected by DQM performed lower than other methods. Regarding EVS, the precipitation
399 corrected by EQM showed the lowest variability, while QDM showed higher variability than
400 EQM but lower variability than DQM.

401 In the case of Pbias, precipitation corrected by DQM was overestimated compared to the
402 reference data throughout Asia. The precipitation corrected by EQM was underestimated in
403 most regions except Central Asia. Precipitation in QDM showed a similar spatial pattern to that
404 in EQM, but the range of Pbias was more diverse.

405



406

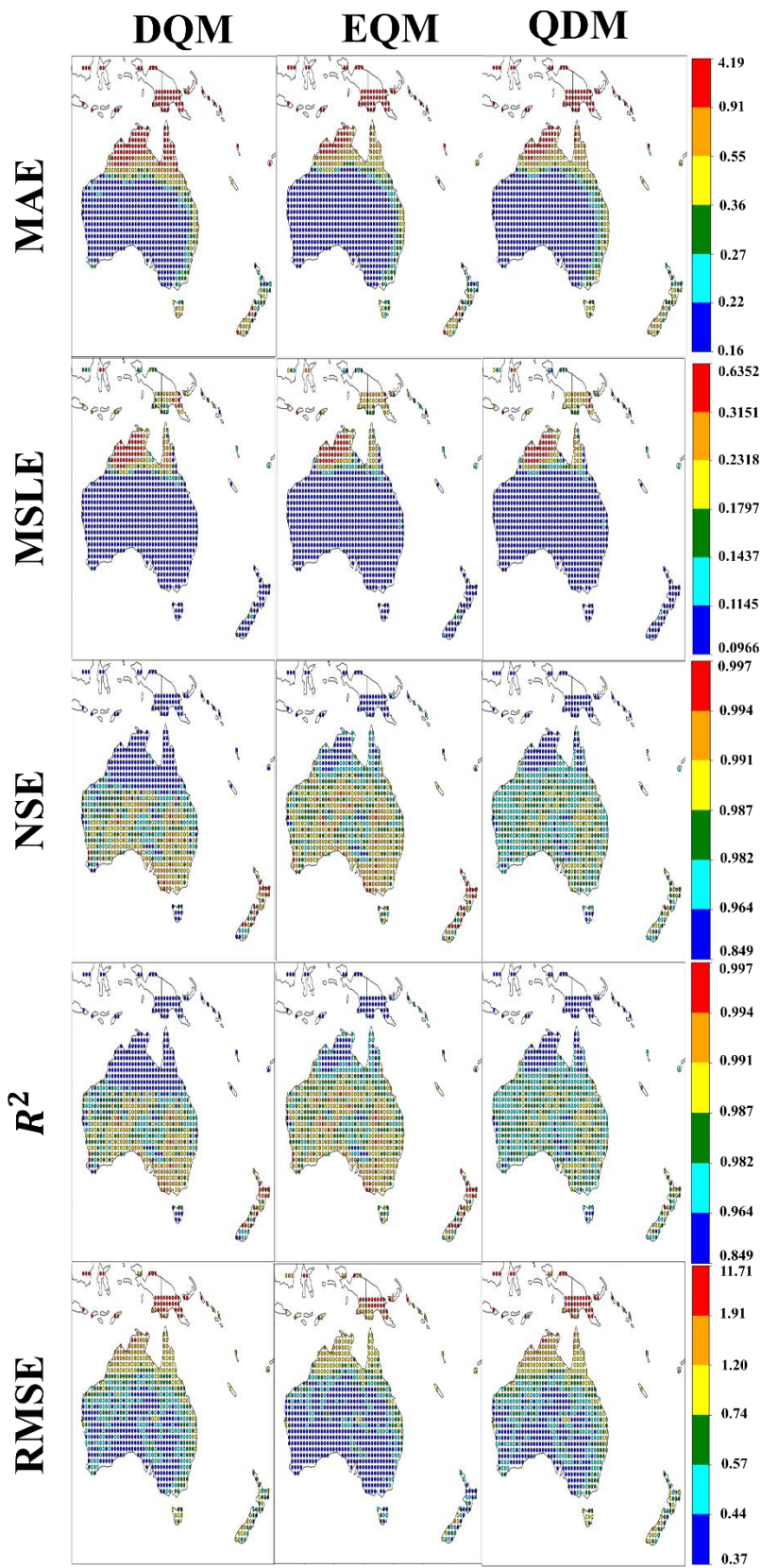
407 Figure 6. Performances of DQM, EQM, and QDM using evaluation metrics (JSD, EVS, MdAE,
 408 Pbias, and KGE) for daily precipitation in Asia.

409

410 Figures 7 and S6 show the results of spatially quantifying the corrected daily precipitation in
 411 Oceania using various evaluation metrics.

412 In terms of error metrics, the precipitation estimated by the three QM methods performed
 413 similarly in MAE, MdAE, and MSLE. However, the precipitation corrected by EQM
 414 performed better in RMSE than the other methods. In the case of JSD, all three methods
 415 performed well.

416 Regarding EVS, the precipitation corrected by EQM showed lower variability than the other
417 methods, and DQM showed higher performance than QDM. In Pbias, the precipitation adjusted
418 by QDM was overestimated compared to the reference data in Oceania, while the precipitation
419 corrected by DQM and EQM was underestimated compared to the reference data in central and
420 southern Oceania. Finally, in KGE, precipitation corrected by EQM showed the highest
421 performance, while DQM showed the lowest performance.



422

423 Figure 7. Performances of DQM, EQM, and QDM using evaluation metrics (MAE, MSLE,

424 NSE, R^2 , and RMSE) for daily precipitation in Asia.

425 Figure 8 visualizes the results of evaluating the bias-corrected precipitation data using 11
426 CMIP6 GCMs on six continents using ten evaluation metrics as boxplots. Overall, the
427 precipitation corrected by EQM outperforms the other methods on most continents. In
428 particular, EQM performs the best on the error metrics. QDM performs slightly lower than
429 EQM but still maintains a high level of performance on all continents. On the other hand, DQM
430 has larger errors and relatively poor performance compared to the other methods on most
431 metrics.



(a) South America (b) North America (c) Africa (d) Europe (e) Asia (f) Oceania

432

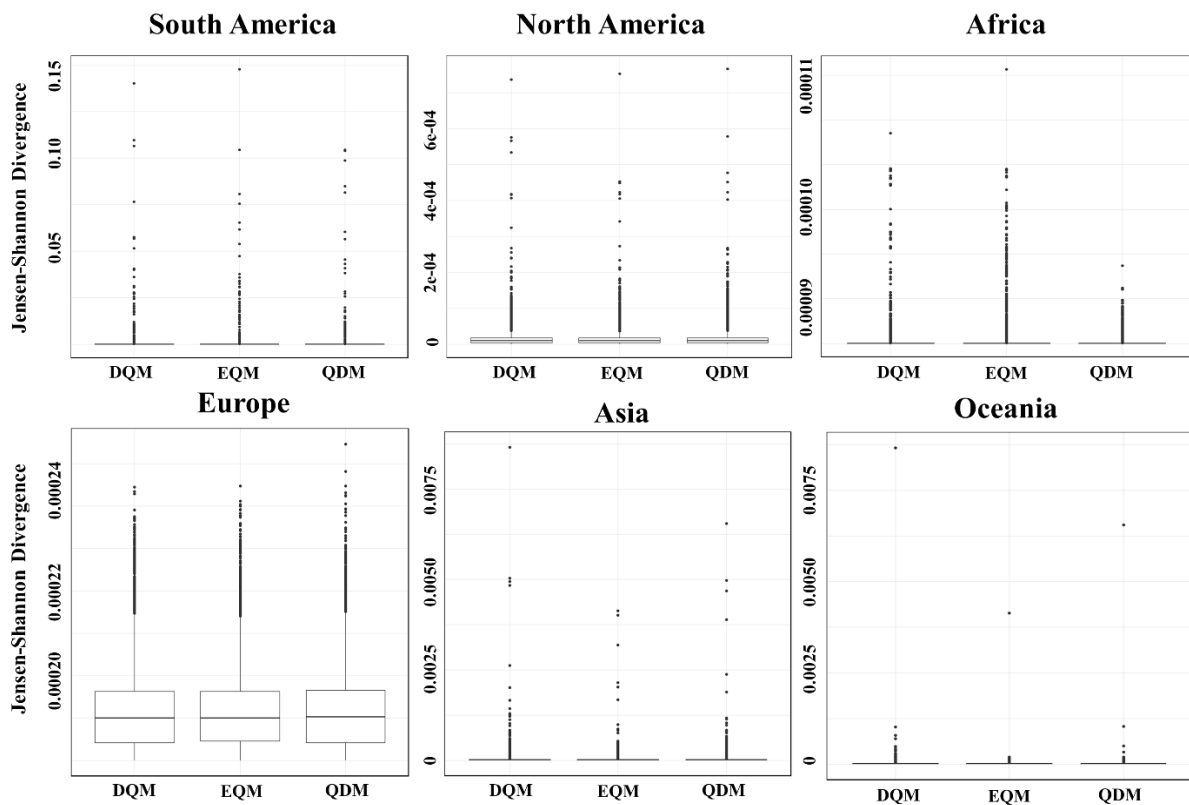
433 Figure 8. Performances of DQM, EQM, and QDM of historical period precipitation using

434 boxplots based on ten evaluation metrics

435

436 **3.1.3 Comparison of reproducibility for extreme daily precipitation**

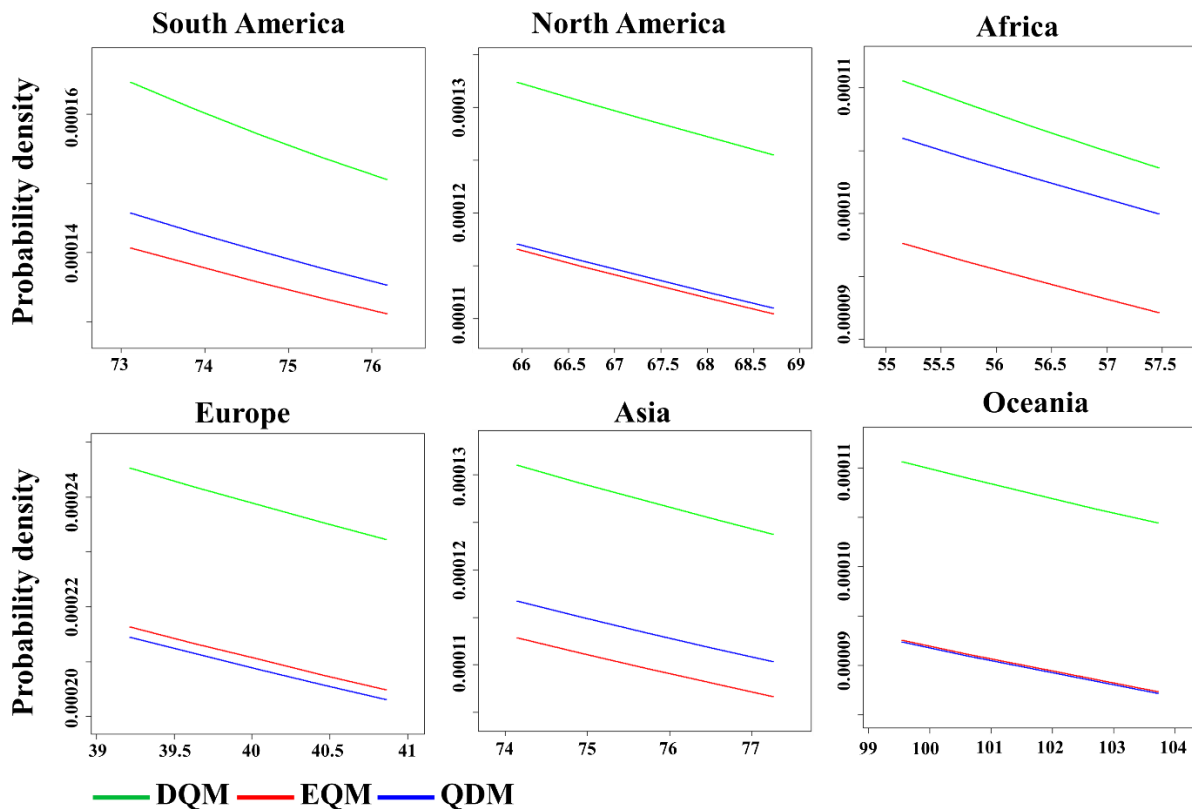
437 This study compared the daily extreme precipitation corrected by three methods using the GEV
438 distribution. Figure 9 compares the distribution differences of the daily precipitation adjusted
439 by the biased bias correction methods based on the GEV distribution using the JSD. In general,
440 the JSD values for precipitation from DQM, EQM, and QDM are very low for most continents,
441 indicating that the GEV distributions are almost identical among the three methods. Although
442 there are some outliers, the overall distribution differences are not large, suggesting that there
443 is little difference among the three methods when correcting for historical precipitation.
444 However, in Europe, unlike other continents, the differences between the 1st and 3rd quartiles
445 of the JSD are relatively significant, indicating that the distributions can vary significantly from
446 grid to grid depending on the QM method.
447



448 Figure 9. Comparison of distribution differences for GEV distribution using JSD across six
449 continents.
450

451
452 Figure 10 shows the probability density functions for extreme precipitation above the 95th
453 percentile of the GEV distribution. Overall, DQM shows the highest probability density for

454 extreme precipitation across all continents and has the widest distribution, indicating that DQM
 455 corrects more extreme precipitation. On the other hand, EQM shows the lowest probability
 456 density and conservatively corrects for extreme precipitation. QDM shows probability
 457 densities between those of EQM and DQM across most continents but closer to EQM.



458
 459 Figure 10. Comparison of probability densities for extreme precipitation values above the 95th
 460 percentile using GEV.

461
 462 **3.2 Prioritization of bias correction methods based on performance**

463 **3.2.1 Results of weight for evaluation metrics**

464 In this study, the weights were calculated by applying entropy theory to the evaluation metrics
 465 used in the TOPSIS analysis, and the results are presented in Table 3. Overall, JSD had the
 466 highest weight in South America because the estimated JSD from 11 CMIP6 GCMs was an
 467 important metric for evaluating model performance differences. These results indicate that the
 468 differences between distributions are large. On the other hand, EVS and NSE in South America
 469 had very low weights, suggesting that the variability and efficiency of precipitation were
 470 considered less important than other indicators. For North America, the RMSE, MSLE, and
 471 MAE metrics were of significant importance, as evidenced by their high weights. These error

472 metrics revealed substantial regional differences. In contrast, EVS carried a negligible weight,
 473 suggesting it was considered less important in explaining variability in North America. For
 474 Africa, MdAE and JSD metrics were of considerable importance, as indicated by their high
 475 weights. These metrics were key evaluation factors in Africa. Conversely, EVS carried a low
 476 weight, suggesting it was considered relatively less important. RMSE had the highest weight
 477 in Europe, and KGE also had a relatively high weight, indicating that these metrics were
 478 considered important evaluation criteria in Europe. In Asia, MAE and MSLE had high weights,
 479 suggesting that these metrics were important evaluation metrics. On the other hand, EVS and
 480 NSE were considered less important due to their low variability. JSD, KGE, RMSE, and MAE
 481 were assigned high weights in Oceania, indicating that these metrics are essential factors. On
 482 the other hand, R^2 and NSE were assigned low weights.

483

484 Table 3. Entropy-based weights for evaluation metrics across different continents

	RMS E	MAE	R^2	NSE	KGE	Pbias	MdAE	MSLE	EVS	JSD
South America	0.1439	0.1536	0.0001	0.0001	0.0005	0.0238	0.1754	0.1934	0.0004	0.3088
North America	0.2289	0.1908	0.0001	0.0001	0.0007	0.0118	0.2152	0.2117	0.0001	0.1411
Africa	0.1319	0.1686	0.0002	0.0002	0.0002	0.0855	0.2436	0.1911	0.0002	0.1786
Europe	0.2821	0.1762	0.0022	0.0022	0.0063	0.0378	0.1754	0.1666	0.0021	0.1490
Asia	0.2073	0.1954	0.00003	0.00003	0.0001	0.0305	0.2300	0.2024	0.00003	0.1342
Oceania	0.2384	0.2204	0.0013	0.0013	0.0068	0.0214	0.2338	0.2093	0.0012	0.0660

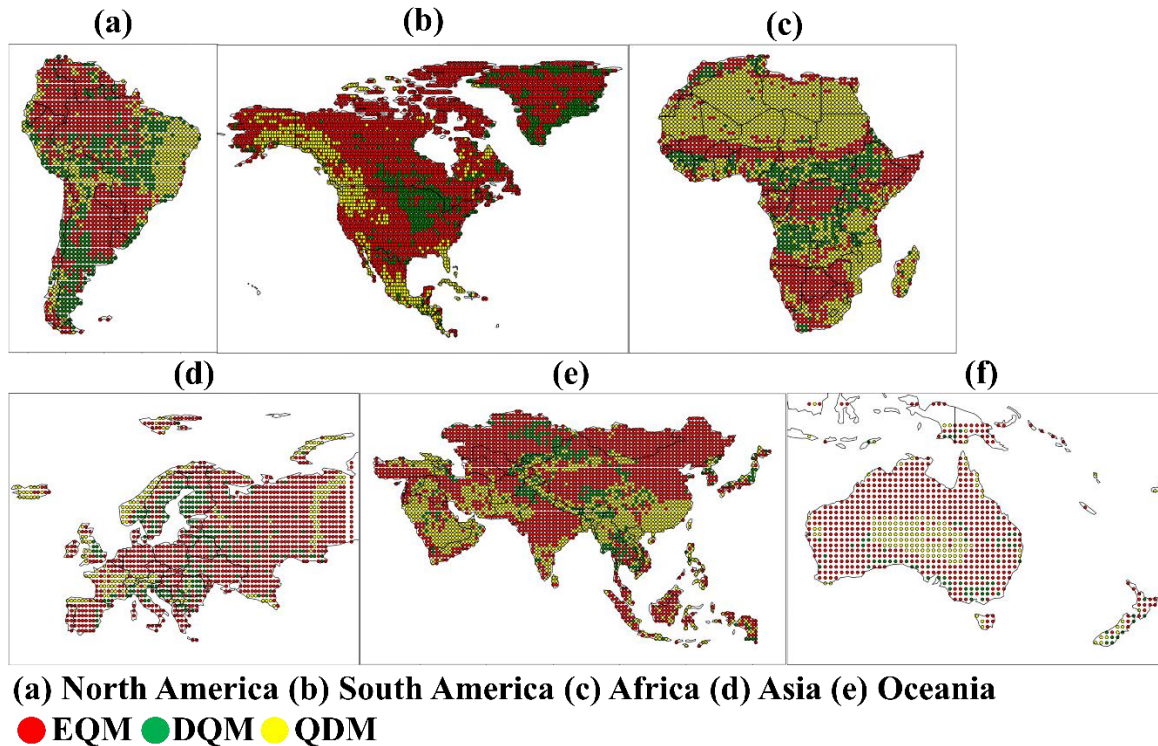
485

486

487 3.2.2 Selection of the best bias correction method based on TOPSIS

488 Figure 11 and S7 presents the best bias correction method selected for each continent using the
 489 TOPSIS approach. In Figure 11(a), the spatial distribution of the most effective bias correction
 490 method across the grid points of each continent is shown. In contrast, Figure 11(b) shows the
 491 number of grid points selected for each QM method. In South America, EQM was chosen as
 492 the best method in most grid points, with EQM being selected in over 1,500 grid points. In
 493 contrast, QDM was selected in fewer than 700 grid cells, making it the least chosen method in
 494 South America. Across all continents except South America, EQM was selected as the best
 495 model in the majority of grid cells, with the number of selected grid points (North America:

496 7,583; Africa: 2,879; Europe: 2,719; Asia: 8,793; and Oceania: 1,659). On the other hand,
 497 DQM was the least chosen method across all continents. For QDM, although it was the second
 498 most selected method across all continents except South America, the difference in the number
 499 of grid points between QDM and EQM is significant.



500
 501 Figure 11 Spatial distribution for selected best bias correction methods across continents
 502 using TOPSIS

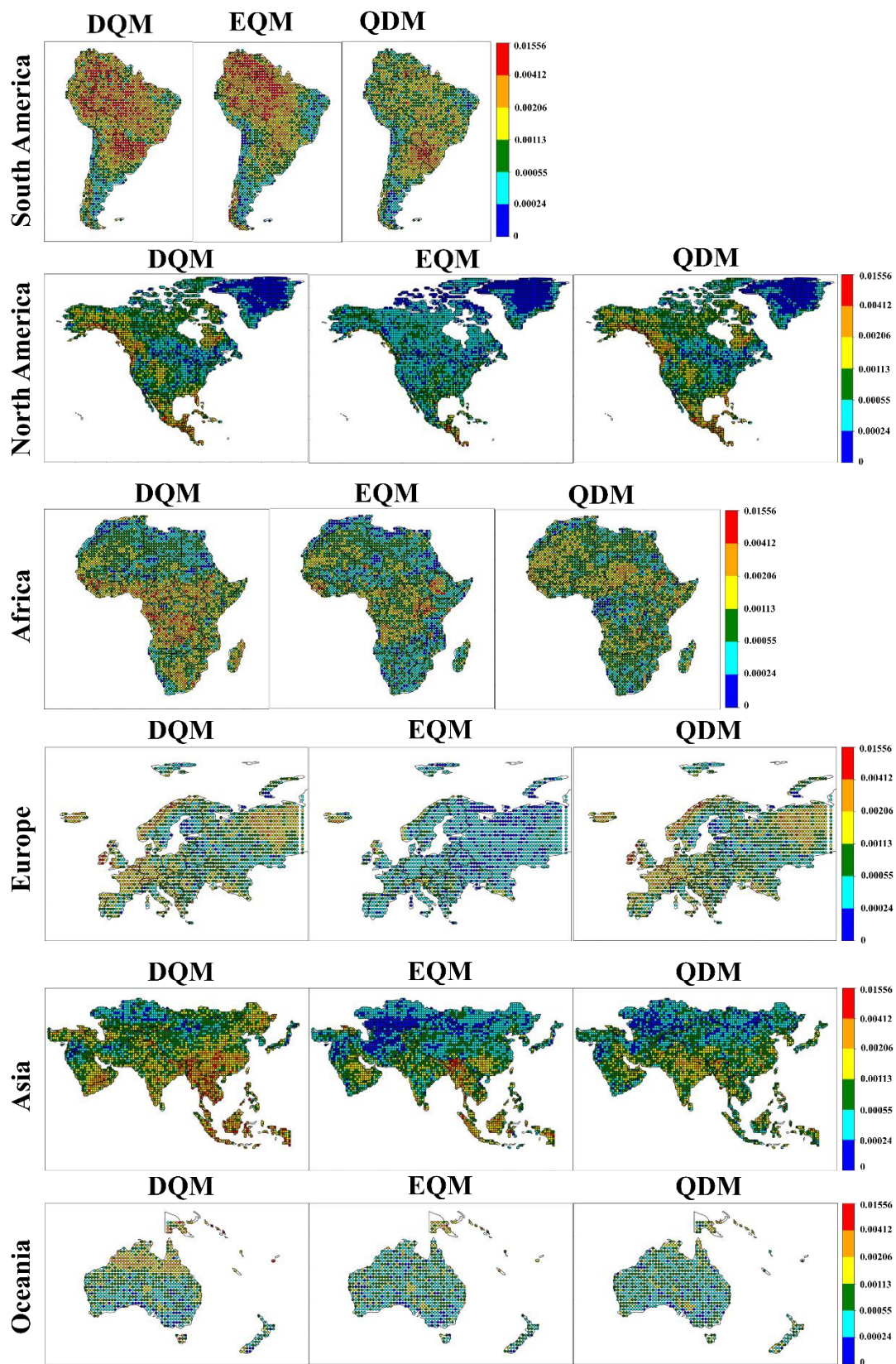
503

504 3.3 Uncertainty quantification of bias corrected daily precipitation

505 3.3.1 Uncertainty by model

506 This study quantifies the daily precipitation uncertainty of 11 CMIP6 GCMs, corrected using
 507 three different methods, using BMA. Figure 12 shows the distribution of GCM weight
 508 variances calculated by BMA across six continents. In South America, the highest weight
 509 variance was observed mainly in DQM. EQM showed high weight variance in the northern
 510 region but lower variance than DQM in most other regions. QDM exhibited the lowest weight
 511 variance, with values less than 0.00113 in most regions. In North America, EQM had the lowest
 512 weight variance, with values between 0.00055 and 0.00024 in most regions. QDM showed the
 513 lowest model uncertainty across North America, with more regions where weight variances
 514 were closer to 0 than the other methods. On the other hand, DQM exhibited high weight

515 variance overall, with exceptionally high model uncertainty in the northeast and southern
516 regions. In Africa, EQM's weight variance was estimated to be low overall, resulting in low
517 model uncertainty in most regions. For QDM, weight variance was low in some regions, but
518 higher than 0.00113 in others. DQM showed high weight variance in most regions except for
519 the northern area, indicating high model uncertainty across the continent. EQM's weight
520 variance was the lowest in Europe compared to the other methods, with weight variances close
521 to 0 across the continent. QDM also showed low weight variance overall, though higher than
522 EQM. DQM exhibited high weight variance in most regions except for Central Europe. In Asia,
523 EQM showed low weight variance in most regions except Southeast Asia. QDM's weight
524 variance was similar to EQM's, though some regions had higher model uncertainty. DQM
525 showed high weight variance in most regions except for some Southwest and North Asian areas.
526 For Oceania, the weight variances of EQM and DQM were mainly similar, but DQM showed
527 a higher weight variance overall.

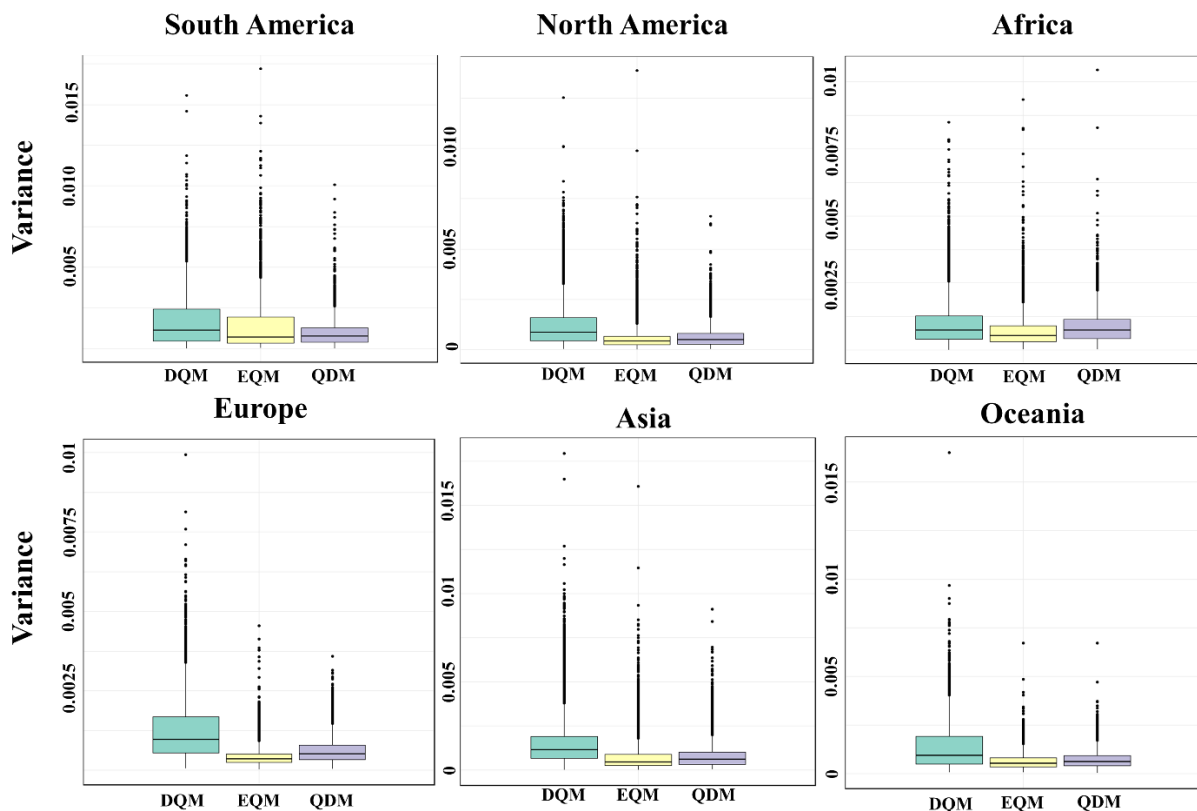


528

529 Figure 12. Spatial distribution of weight variance across continents for bias corrected CMIP6

530 GCMs using BMA

531 Figure 13 shows the distribution of GCM weight variances calculated using BMA across six
 532 continents, presented as boxplots. Overall, EQM has the smallest weight variance, and QDM
 533 has the second smallest weight variance on all continents except South America. In contrast,
 534 in South America, QDM has the smallest weight variance, and EQM has the second smallest.
 535 DQM consistently has the largest weight variance across all continents, indicating the highest
 536 model uncertainty.
 537

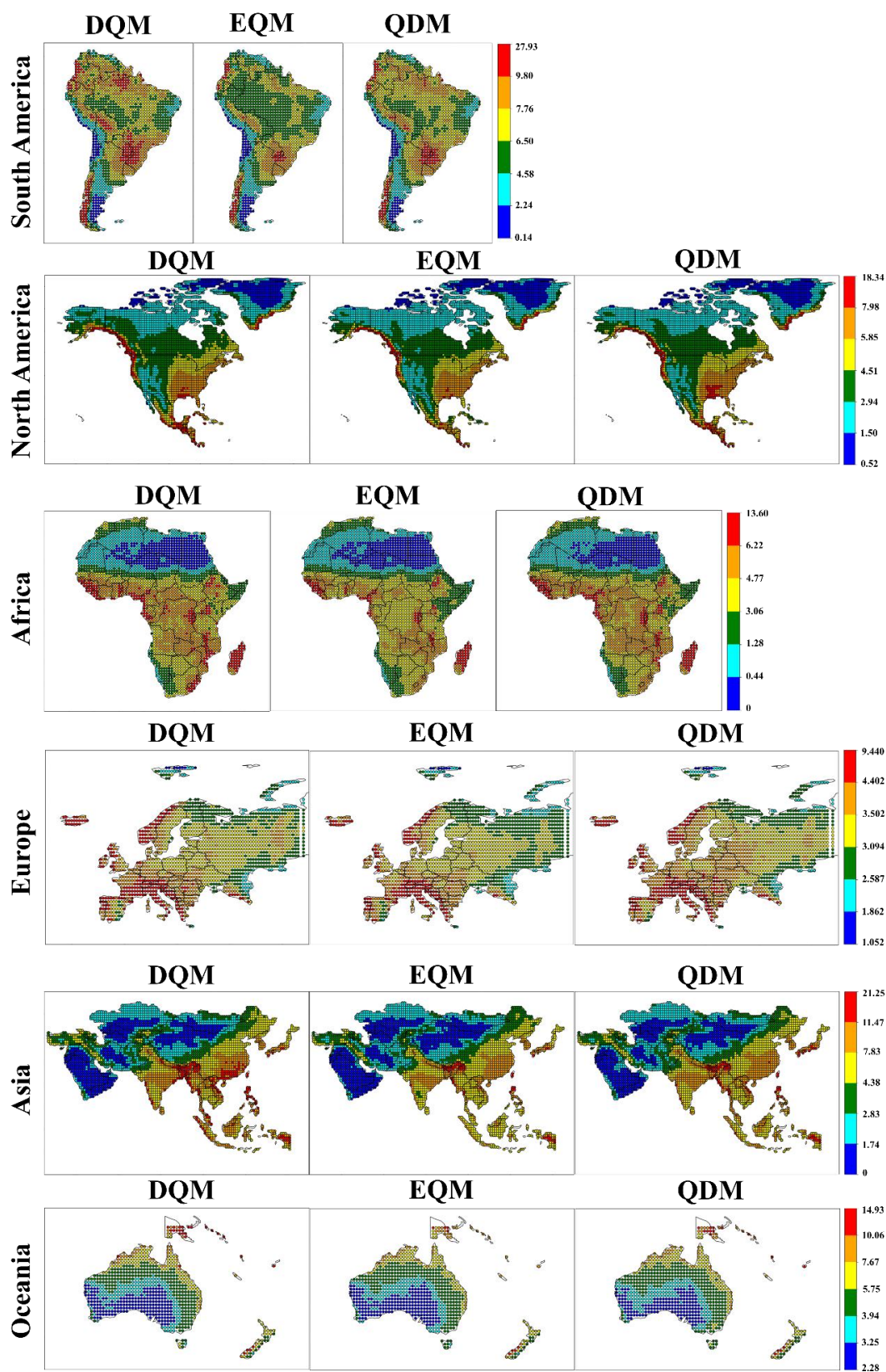


538
 539 Figure 13. Weight variance for bias correction methods across six continents using box plots.
 540

541 3.3.2 Uncertainty by ensemble prediction

542 This study developed a daily precipitation ensemble for the historical period based on 11
 543 CMIP6 GCMs using BMA. Figure 14 shows the standard deviation of daily precipitation for
 544 the historical period by continent for the ensemble developed using BMA with 11 CMIP6
 545 GCMs. Overall, the ensemble predicted using EQM provided stable precipitation projection
 546 with low standard deviations across most continents. The QDM ensemble showed similar
 547 results to EQM for most continents except Oceania, but the standard deviations were slightly
 548 higher. On the other hand, the ensemble using DQM exhibited higher standard deviations than

549 the other methods for all continents and had the largest prediction uncertainty. In Oceania, the
550 ensembles predicted by the three methods showed similar results. However, the prediction
551 uncertainty was estimated to be lower in the order of EQM, DQM, and QDM due to slight
552 differences.



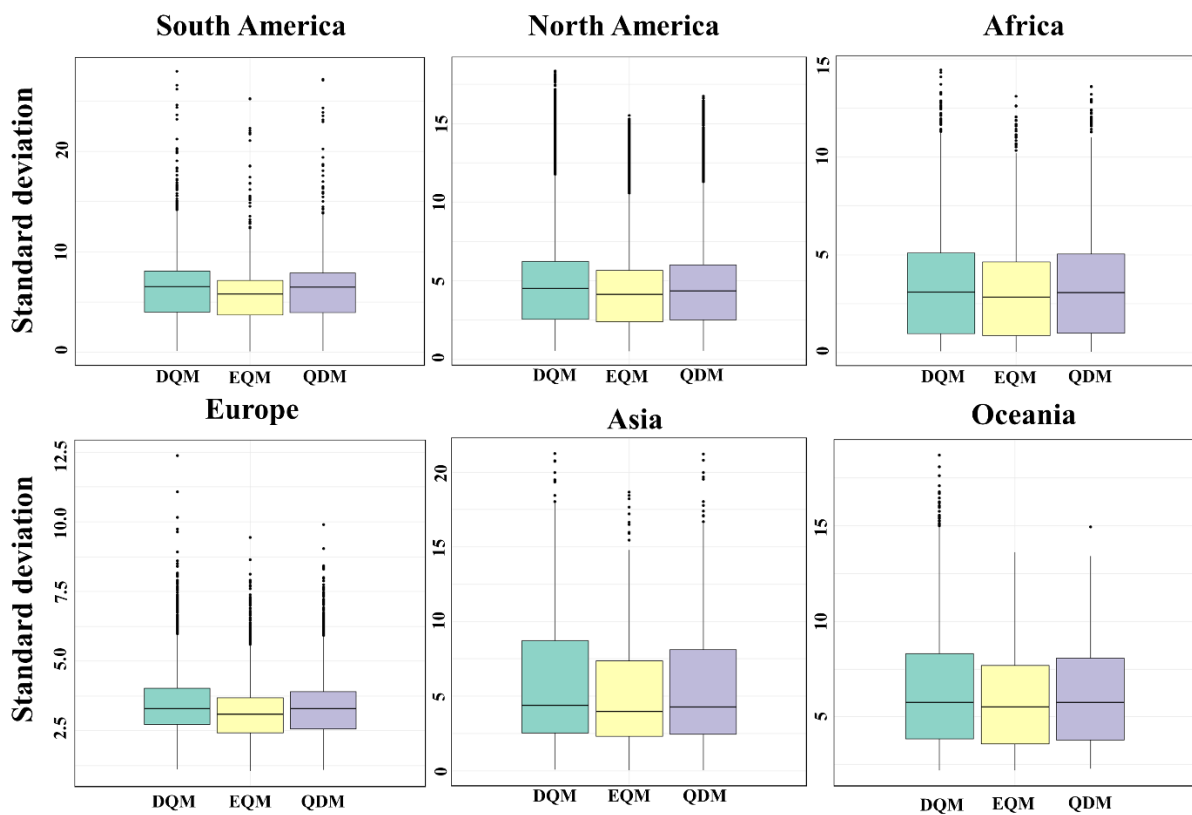
553

554 Figure 14. Spatial distribution of standard deviation for daily precipitation across continents

555 for bias corrected CMIP6 GCMs using BMA

556
557
558
559
560
561
562
563
564

Figure 15 shows the standard deviation of daily precipitation for the ensemble forecasted by BMA using three methods, DQM, EQM, and QDM, in a boxplot for each continent. Overall, the EQM ensemble showed the lowest standard deviation across all continents, providing the most stable daily precipitation forecasts. The QDM ensemble showed slightly higher standard deviations than EQM for most continents, but there was no significant difference between the two methods. In contrast, the ensemble using DQM showed the highest standard deviation and the largest prediction uncertainty.



565
566
567
568

Figure 15. Spatial distribution of standard deviation for daily precipitation across continents for bias corrected CMIP6 GCMs using BMA

569 3.4 Evaluation of bias correction methods using CI

570 3.4.1 Results of CI by each weighting case

571 This study compared three QM methods by generating a CI based on three cases of weighting
572 values that considered both model performance and uncertainty. Figures 16, S8, and S9 show

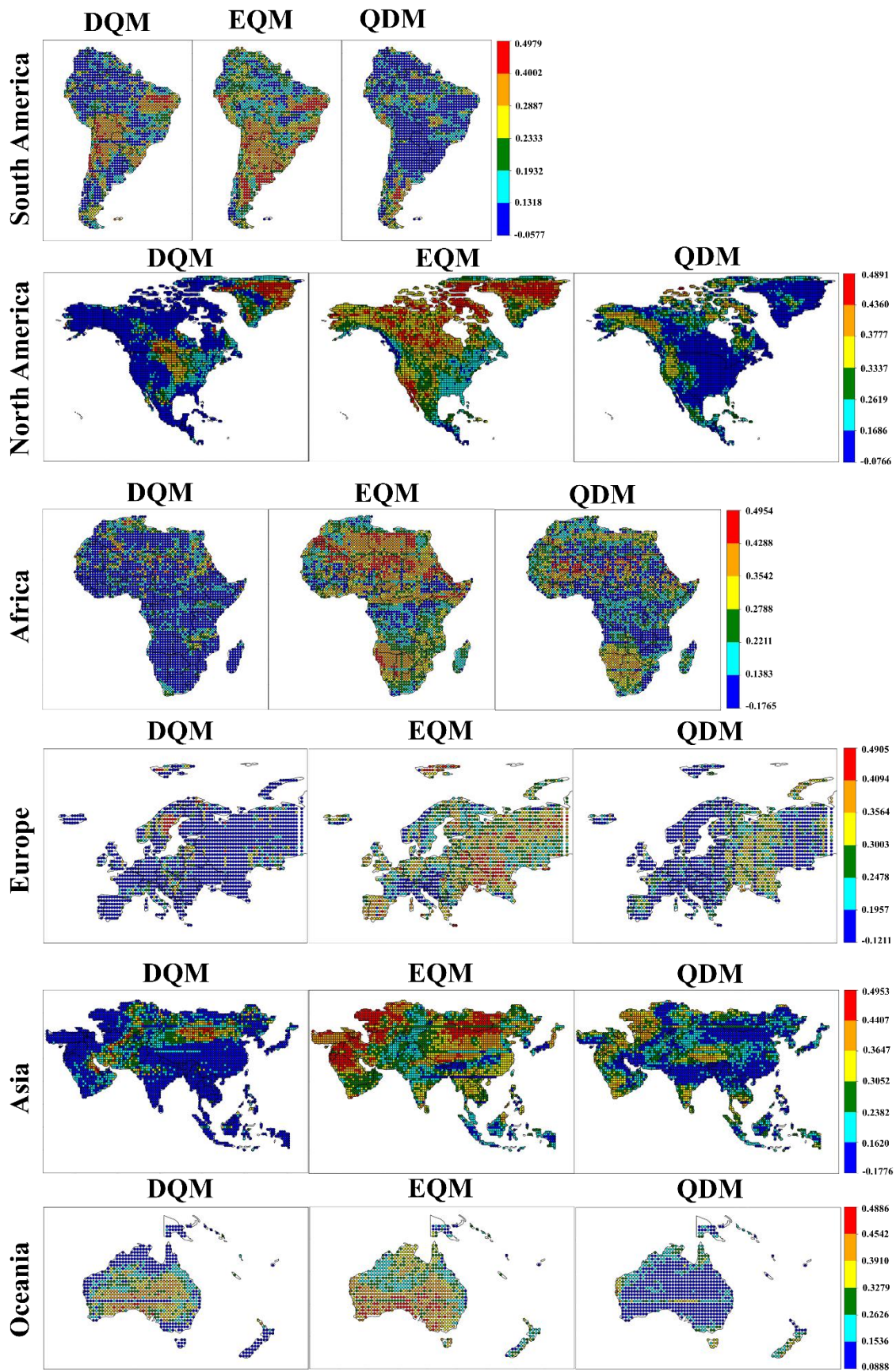
573 the comprehensive indices calculated by applying equal weights, weights that emphasize
574 performance, and weights that emphasize uncertainty, respectively.

575 When equal weights were applied, EQM showed the highest CI across all continents. However,
576 the index was lower in southern Europe and southeastern North America, but it calculated high
577 values in most other regions. QDM showed high index values in some regions, although it was
578 lower than EQM. For example, the CI results were high in the northern and western parts of
579 North America and the central part of Europe. On the other hand, DQM was generally
580 unsuitable in most regions but showed a relatively high index in Oceania.

581 When weights that emphasized performance were applied, DQM showed a high index in the
582 central part of South America but low performance in most continents. Nevertheless, DQM
583 showed a better index than QDM in some parts of Oceania. EQM showed the best index across
584 most continents. While QDM was less suitable than EQM, it was still evaluated as a useful
585 method in some continents.

586 Even when applying weights that increased the emphasis on uncertainty, similar results were
587 obtained with the other weighting values. In particular, EQM was evaluated as the most suitable
588 model across all continents, while DQM showed the opposite results.

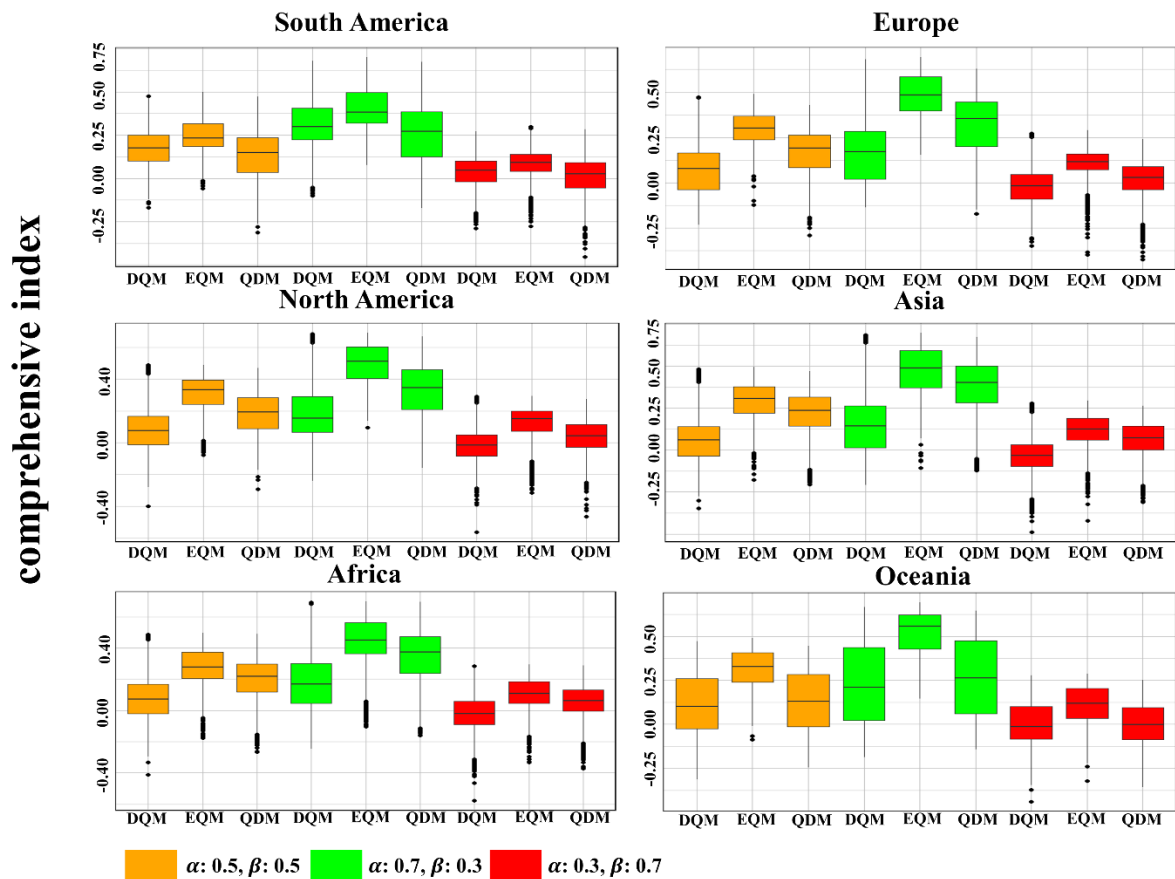
589



591 Figure 16. Spatial distribution of comprehensive indices for bias correction methods with equal
 592 weights ($\alpha: 0.5, \beta: 0.5$) across continents

593

594 Figure 17 presents a comparison of the comprehensive indices for three QM methods with
 595 different weights for each continent using box plots. Overall, all methods showed absolutely
 596 higher indices than the other weighting values in the values that emphasized more weight on
 597 performance. In all weighted values, DQM showed the lowest indices in all continents except
 598 for South America and Oceania, where it was slightly higher or similar to QDM. EQM showed
 599 the best composite indices in all continents, outperforming both performance and uncertainty.
 600 QDM showed high comprehensive indices in most continents, and the gap with EQM narrowed
 601 significantly in the weighting values that emphasized performance more. Nevertheless, QDM
 602 overall had lower comprehensive indices than EQM.
 603



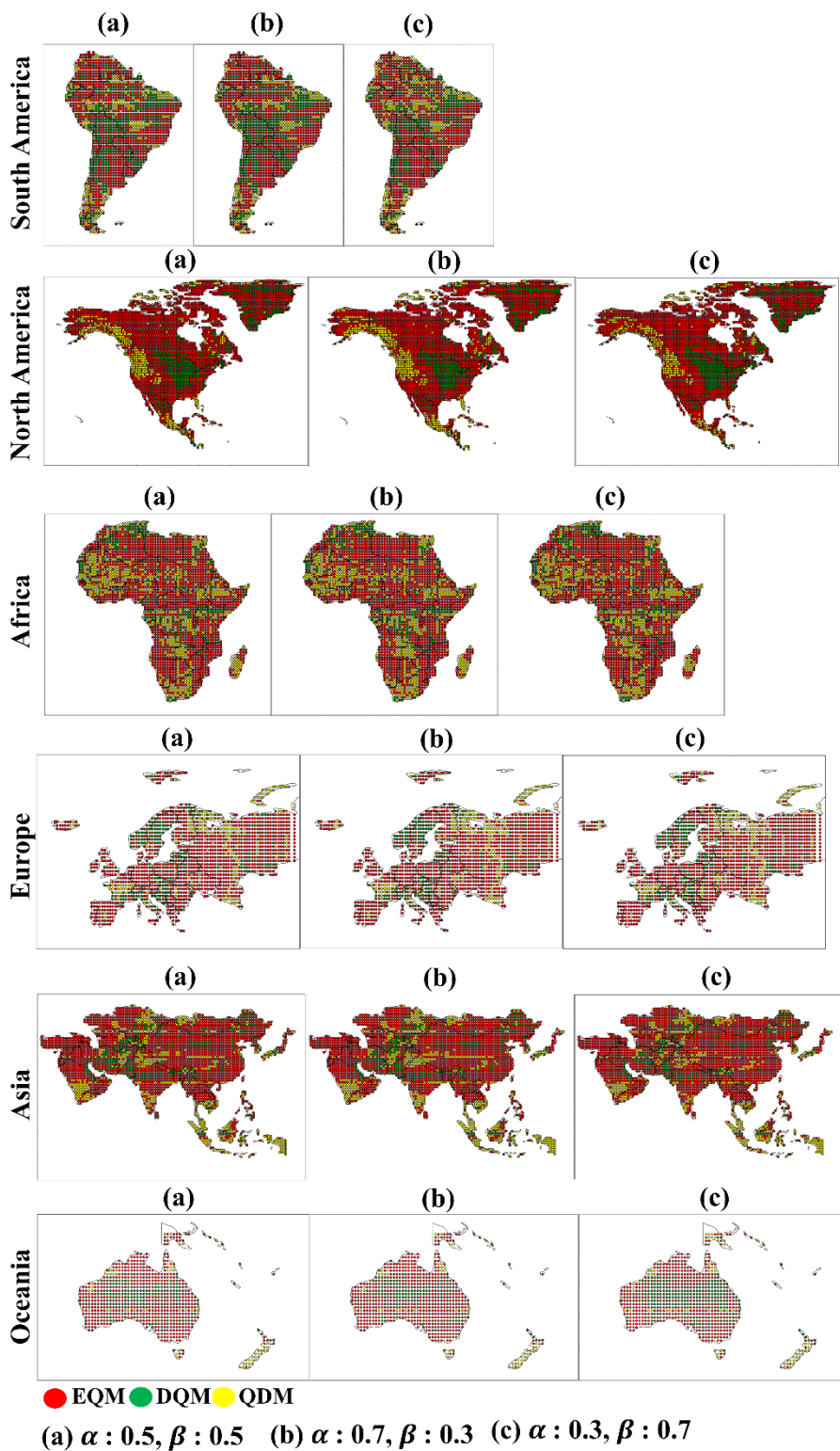
604

605 Figure 17. CI for three bias correction methods across continents with varying weights on
 606 performance and uncertainty

607

608 **3.4.2 Selection of best bias correction method**

609 This study selected the best bias correction method for each continent based on the CI. Figure
610 18 shows how the best bias correction method was selected for each continent by applying
611 various weighting values of the CI. Overall, EQM was selected as the best correction method
612 for most continents in all weighting values and was selected more than other methods in North
613 America, Europe, Asia, and Oceania. DQM was selected the least in most continents except
614 for South America and Oceania, and the number of selected grids tended to decrease as the
615 weighting for uncertainty increased. QDM was selected as the proper bias correction method
616 in western North America, southern and eastern Africa, and northern Europe. In addition, QDM
617 was selected the most in Southeast Asia in all weighting values.

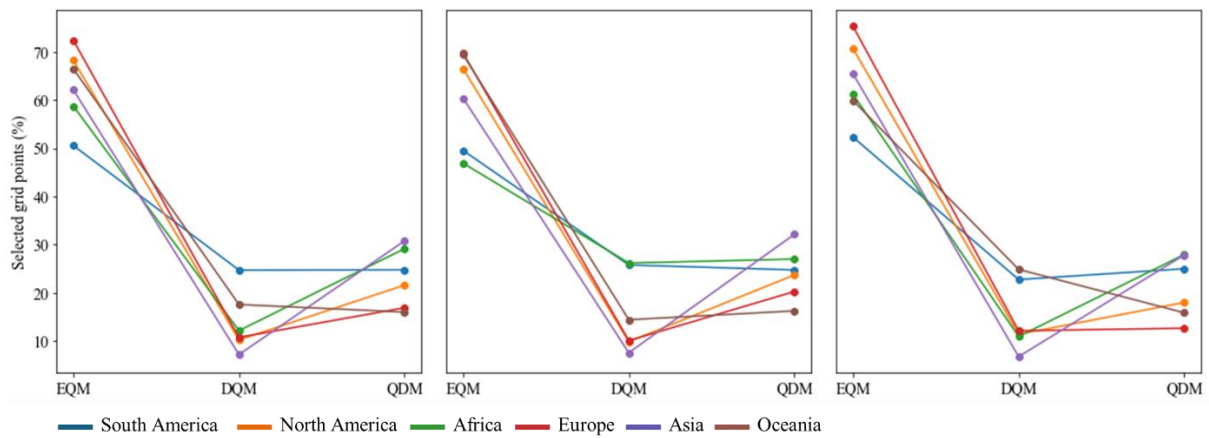


618

619 Figure 18. Selection of best bias correction methods across continents based on CI depending
 620 on weighting values.

621

622 Figure 19 shows the number of selected grids for the best bias correction method across
 623 continents based on three weighting values. Overall, EQM was the most frequently selected
 624 method across all weighting values, demonstrating superior performance across all continents
 625 compared to the other methods. Interestingly, as the weight for uncertainty increased, the
 626 number of grids where EQM was selected also increased, while the number decreased as the
 627 weight for performance increased. In contrast, QDM was chosen as the second-best method on
 628 most continents, except for South America and Oceania. The number of selected grids for
 629 QDM slightly increased as the performance weight increased. DQM was the least selected
 630 method across most continents, indicating that it was the least suitable overall.
 631



632
 633 Figure 19. Ratios of selected grids for best bias correction methods across continents based on
 634 different weighting values
 635

636 4. Discussion

637 Bias correction methods are widely used in correcting GCM outputs, and previous studies have
 638 compared the performance of various methods (Homsí et al., 2019; Saranya and Vinish, 2021).
 639 Among these, Quantile Mapping (QM) has consistently shown superior performance compared
 640 to other methods, making it a widely used approach for bias correction. In particular, QDM,
 641 EQM, and DQM, which are the focus of this study, are frequently employed in research
 642 exploring and applying climate change projections based on GCM outputs (Cannon et al., 2015;
 643 Switanek et al., 2016; Song et al., 2022a). Analyzing the strengths and limitations of these three
 644 methods will provide valuable insights for climate researchers, enabling them to choose the
 645 most suitable bias correction method for specific regions. In this context, this study further
 646 evaluates the performance of QDM, EQM, and DQM, especially for daily precipitation, and

647 investigates how these methods perform across different regions. This section discusses the
648 strengths and weaknesses of each method from various perspectives to provide a more balanced
649 assessment.

650

651 **4.1 Evaluation of bias correction methods performance**

652 The daily precipitation corrected by the three QM methods outperformed the raw GCM data
653 (see Figure 1). All three methods showed strong overall performance, as indicated by the
654 Taylor diagram, producing consistently good results across different regions. This highlights
655 the need to use multiple performance metrics to fully understand the strengths and weaknesses
656 of the three QM methods, as relying on a single analysis or macroscopic perspective can
657 overlook important details. From this perspective, many studies have emphasized the
658 application of a multifaceted analysis in selecting bias correction methods (Homsí et al., 2019;
659 Cannon et al., 2015; Berg et al., 2022; Song et al., 2023). The spatial distribution of correction
660 performance, as discussed in Section 3.1.2, varies significantly by continent. Figures 2 to 7
661 reveal that the evaluated metrics differ across continents, underscoring the importance of
662 region-specific correction methods. This finding aligns with Song et al. (2023), highlighting
663 the importance of selecting appropriate correction methods based on the precipitation
664 distribution at observation sites. Moreover, studies such as Homsí et al. (2019) and Saranya
665 and Vinish (2021) also emphasize the variability in bias correction performance depending on
666 the regional climate and data characteristics, reinforcing the need for tailored approaches. For
667 example, the three QM methods tend to perform less effectively in regions with high
668 precipitation, but their performance also varies by grid (e.g., southern India in Asia: RMSE;
669 central Oceania: Pbias and EVS; central Europe: Pbias, MdAE, and KGE). While EQM
670 performs well across most continents, DQM and QDM show superior results in specific regions.
671 Similar results were made by Cannon et al. (2015), which highlighted differences in the
672 performance of bias correction methods, particularly in handling extreme precipitation events.
673 QDM's error-related metrics (South America: RMSE, MAE, and MSLE) are nearly identical
674 to EQM's, yet QDM outperforms EQM regarding MdAE on more grids. These findings suggest
675 that a more nuanced and detailed analysis of precipitation corrected by GCMs is necessary,
676 aligning with the conclusions of Gudmundsson et al. (2012), which emphasize that the
677 effectiveness of bias correction methods can vary significantly depending on local climate
678 characteristics, highlighting the importance of selecting appropriate methods for each region.

679 These results suggest that a more detailed analysis of precipitation from corrected GCMs is
680 needed.

681 This study compared the three QM methods for daily precipitation events above the 95th
682 percentile (extreme precipitation) using the GEV distribution, as shown in Figure 10. The
683 results indicate that DQM tends to correct more extreme precipitation events than QDM,
684 aligning with previous findings that DQM captures a broader range of extremes. At the same
685 time, QDM and EQM take a more conservative approach (as noted in previous studies such as
686 Cannon et al., 2015). These findings suggest that EQM and QDM may be more suitable in
687 regions vulnerable to floods and extreme weather events that require a more balanced and
688 cautious approach. However, when comparing the differences in GEV distributions, there was
689 no significant difference between methods in regions like Oceania and Europe (see Figure 9).
690 These results imply that EQM can better handle extreme values or outliers in the data by
691 directly comparing and correcting past and future distributions. In particular, EQM is consistent
692 with previous studies in that it more accurately corrects observed distributions in non-stationary
693 and highly variable climate variables, such as precipitation (Themeßl et al., 2012; Maraun,
694 2013; Gudmundsson et al., 2012). Although there are significant advantages in observing the
695 results of the correction method in detail from various perspectives, presenting these results
696 without integrating them into a reasonable framework can increase confusion and uncertainty
697 in climate change research (Wu et al., 2022). Therefore, it is essential to introduce a structured
698 framework such as MCDA to provide a single integrated result.

699

700 **4.2 Uncertainties of model and ensemble prediction in bias correction methods**

701 In climate modeling, quantifying uncertainty is essential to assess the reliability of bias-
702 corrected precipitation data. This study applied BMA to quantify the uncertainty of three QM
703 methods on a continental basis, addressing both model-specific and ensemble prediction
704 uncertainties. Similar to the findings by Cannon et al. (2015), this analysis demonstrates how
705 different bias correction methods yield varying uncertainty levels based on the underlying
706 climate models. Notably, EQM showed the lowest weight variance across most continents,
707 which means that the inter-model uncertainty for 11 GCMs corrected by EQM is lower than
708 that of the other QM methods. The low uncertainty associated with EQM aligns with previous
709 studies like Themeßl et al. (2012), which found that EQM consistently reduced discrepancies
710 between modeled and observed data across regions. EQM's ability to manage extreme

711 precipitation and anomalous values based on observed distributions contributes to its reliability,
712 a feature also emphasized by Gudmundsson et al. (2012). On the other hand, DQM showed the
713 highest weight variance across all continents, indicating more significant uncertainty when
714 applied to various GCMs. This uncertainty was particularly pronounced in regions with
715 complex climate conditions, such as Southeast Asia, East Africa, and the Alps in Europe. These
716 results align with Berg et al. (2022), who highlighted DQM's limitations in capturing long-term
717 climate trends and extreme events. The higher uncertainty associated with DQM suggests that,
718 while its detrending process is effective in correcting the mean, it may struggle in regions
719 dominated by nonlinear climate patterns, as it does not sufficiently account for all quantiles in
720 the distribution, particularly extremes, as noted by Cannon et al. (2015). QDM, though showing
721 lower weight variance than DQM, still demonstrated higher uncertainty than EQM in regions
722 with diverse climate characteristics. These results are consistent with the study of Tong et al.
723 (2021), suggesting that QDM performs better under moderate precipitation scenarios. However,
724 the uncertainty may increase under highly variable or extreme weather conditions. Furthermore,
725 this study extended the uncertainty analysis to ensemble predictions, calculating the standard
726 deviation of daily precipitation for each continent using BMA. The EQM-based ensemble
727 consistently exhibited low standard deviations across all continents, indicating that EQM offers
728 the most stable and reliable precipitation predictions. This finding echoes the conclusions
729 drawn by Teng et al. (2015), where EQM provided more accurate and less uncertain projections.
730 In contrast, DQM presented the most significant prediction uncertainty, reinforcing the need
731 for caution when applying DQM in studies that require high-confidence data. These results
732 emphasize the importance of weighing both performance and uncertainty when choosing a
733 suitable bias correction method. EQM's consistent performance in reducing uncertainty across
734 both model-specific and ensemble forecasts highlights its robustness as a preferred choice for
735 climate research. However, the substantial uncertainty associated with DQM suggests that its
736 use should be limited to regions where its detrending process can be beneficial. Overall, these
737 findings stress the critical role of uncertainty quantification in climate change impact
738 assessments and underscore the need for selecting bias correction methods based on a
739 comprehensive evaluation of both performance and uncertainty.

740

741 **4.3 Integrated assessment of bias correction methods**

742 This study selected the optimal QM method for each continent based on the CI, which considers
743 uncertainty and performance. The critical point is that uncertainty is decisive when selecting a
744 bias correction method. As shown in Figure 19, the optimal correction method varies depending
745 on the continent, and the selected method also changes depending on the weight. These results
746 suggest that uncertainty still exists, as Berg et al. (2022) pointed out, and that uncertainty must
747 be considered when selecting the optimal method. In other words, even if the QM method has
748 high performance, it is difficult to make a reasonable selection if the uncertainty contained in
749 the method is significant. Overall, EQM showed the highest CI value in all continents, which
750 means that it provides the most balanced results in terms of performance and uncertainty. These
751 results are consistent with previous studies (Lafon et al., 2013; Teutschbein and Seibert, 2012;
752 Teng et al., 2015) that showed high precipitation correction accuracy and excellent
753 performance, especially under complex climate conditions. QDM was evaluated highly in some
754 regions but performed worse than EQM overall. Berg et al. (2022) also pointed out that QDM
755 is superior in general climate conditions but may perform worse in extreme climate situations,
756 suggesting that this may increase the uncertainty of QDM in extreme climates. DQM was
757 evaluated as an unsuitable method in most regions due to low CI values, which is consistent
758 with the limitations of DQM mentioned in Cannon et al. (2015) and Berg et al. (2022). It was
759 confirmed that DQM performs relatively well in dry climates but may perform worse in various
760 climate conditions. In addition, some differences were observed with the results based on
761 TOPSIS. For example, DQM was selected more than QDM in South America, but when the
762 uncertainty weight was applied, QDM was selected more. Conversely, in Oceania, QDM was
763 selected more than DQM, but when the uncertainty weight was increased to 0.7, DQM was
764 selected more. These results are consistent with those of Lafferty and Sriver (2023), showing
765 that when significant uncertainty exists, uncertainty can be greater despite high bias correction
766 performance. In conclusion, EQM is the most balanced method regarding performance and
767 uncertainty and will likely be preferred in future climate modeling studies. However, there may
768 be more suitable QM methods depending on the region, and a comprehensive evaluation with
769 various weights is needed. Therefore, when establishing climate change response strategies or
770 policy decisions, it is essential to take a multifaceted approach that considers uncertainty
771 together rather than relying on a single indicator or performance alone. It will enable more
772 reliable predictions and better decision-making.

773

774 **5. Conclusion**

775 This study corrected and compared historical daily precipitation from 11 CMIP6 GCMs using
776 three QM methods. Eleven statistical metrics were used to evaluate the performance of the
777 precipitation corrected by three QM methods, and TOPSIS was applied to select performance-
778 based priorities. BMA was applied to quantify model-specific and ensemble prediction
779 uncertainties. Additionally, suitable QM methods were selected and compared using a CI that
780 integrates TOPSIS performance scores with BMA uncertainty metrics. The conclusions of this
781 study are as follows:

- 782 1. EQM showed the highest overall index across all continents, indicating that it provides
783 the most balanced approach in terms of performance and uncertainty.
- 784 2. DQM effectively reproduced the dry climate in North Africa and parts of Central and
785 Southwest Asia but showed the highest uncertainty across all continents. These results
786 suggest that DQM may lose some long-term trend information, making it less reliable
787 in regions prone to extreme weather events.
- 788 3. QDM performed better in certain regions, such as Southeast Asia, and was selected
789 more often than DQM when uncertainty was given greater weight. QDM may be a
790 promising alternative in areas where uncertainty plays a significant role.
- 791 4. Selecting an appropriate QM is required for high performance, and significant
792 uncertainty can complicate rational decision-making. Therefore, a multifaceted
793 approach considering performance and uncertainty is essential in climate modeling.

794 In conclusion, EQM has emerged as the preferred method due to its balanced performance, but
795 this study emphasizes the importance of regional assessment and careful consideration of
796 uncertainty when selecting a QM method. Future research should integrate greenhouse gas
797 scenarios to improve the accuracy of climate predictions and provide a more comprehensive
798 understanding of future climate risks.

799

800 **Code availability**

801 Codes for benchmarking the xclim of python package are available from
802 <https://xclim.readthedocs.io/en/stable/>. Furthermore, the Comprehensive Index proposed in
803 this study, along with the performance and uncertainty indices used within it, is available at
804 <https://doi.org/10.6084/m9.figshare.27987665.v2> (Song, 2024).

805

806 **Data availability**

807 The data used in this study are publicly available from multiple sources. CMIP6 General
808 Circulation Models (GCMs) outputs were obtained from the Earth System Grid Federation
809 (ESGF) data portal at <https://esgf-node.llnl.gov/search/cmip6/>. Users can select data types such
810 as climate variables, time series, and experiment ID, which can be downloaded as NC files.
811 Furthermore, CMIP6 GCMs output can also be accessed in Eyring et al. (2016) The ERA5
812 reanalysis dataset used in this study is available through the Copernicus Data Store (CDS)
813 provided by ECMWF ([https://cds.climate.copernicus.eu/cdsapp#!/dataset/reanalysis-era5-
814 single-levels?tab=overview](https://cds.climate.copernicus.eu/cdsapp#!/dataset/reanalysis-era5-single-levels?tab=overview)). ERA5 is available at <https://doi.org/10.24381/cds.bd0915c6>
815 (Hersbach et al., 2023).

816

817 **Author contributions**

818 Young Hoon Song: Conceptualization, Methodology, Data curation, Funding acquisition,
819 Visualization, Writing – original draft, Writing – review & editing. Eun Sung Chung: Formal
820 analysis, Funding acquisition, Methodology, Project administration, Supervision, Validation,
821 Writing-review & editing

822

823 **Declaration of Competing Interests**

824 The authors declare that they have no known competing financial interests or personal
825 relationships that could have appeared to influence the work reported in this paper.

826

827 **Acknowledgement**

828 This study was supported by National Research Foundation of Korea (NRF) (RS-2023-
829 00246767_2; 2021R1A2C200569914)

830

831 **Reference**

- 832 1. Abdelmoaty, H.M., and Papalexiou, S.M.: Changes of Extreme Precipitation in
833 CMIP6 Projections: Should We Use Stationary or Nonstationary Models? *J. Clim.*
834 36(9), 2999-3014, <https://doi.org/10.1175/JCLI-D-22-0467.1>, 2023.
- 835 2. Ansari, R., Casanueva, A., Liaqat, M.U., and Grossi, G.: Evaluation of bias
836 correction methods for a multivariate drought index: case study of the Upper Jhelum
837 Basin. *GMD* 16(7), 2055-2076, <https://doi.org/10.5194/gmd-16-2055-2023>, 2023.

- 838 3. Berg P., Bosshard, T., Yang, W., and Zimmermann, K.: MIdASv0.2.1 – Multi-scale
839 bias AdjuStment. *GMD* 15, 6165-6180, <https://doi.org/10.5194/gmd-15-6165-2022>,
840 2022
- 841 4. Cannon, A. J., Sobie, S. R., and Murdock, T.Q.: Bias correction of GCM
842 precipitation by quantile mapping: How well do methods preserve changes in
843 quantiles and extremes? *J. Clim.* 28(17), 6938-6959, [https://doi.org/10.1175/JCLI-D-](https://doi.org/10.1175/JCLI-D-14-00754.1)
844 14-00754.1, 2015.
- 845 5. Cannon, A.J.: Multivariate quantile mapping bias correction: an N-dimensional
846 probability density function transform for climate model simulations of multiple
847 variables. *Clim. Dyn.* 50, 31–49. <https://doi.org/10.1007/s00382-017-3580-6>, 2018.
- 848 6. Chae, S. T., Chung, E. S., and Jiang, J.: Robust siting of permeable pavement in
849 highly urbanized watersheds considering climate change using a combination of
850 fuzzy-TOPSIS and the VIKOR method. *Water Resour. Manag.* 36(3), 951–969,
851 <https://doi.org/10.1007/s11269-022-03062-y>, 2022.
- 852 7. Chua, Z.W., Kuleshov, Y., Watkins, A.B., Choy, S., and Sun, C.: A Comparison of
853 Various Correction and Blending Techniques for Creating an Improved Satellite-
854 Gauge Rainfall Dataset over Australia. *Remote Sens.* 14(2), 261,
855 <https://doi.org/10.3390/rs14020261>, 2022.
- 856 8. Chung, E. S., and Kim, Y.J.: Development of fuzzy multi-criteria approach to
857 prioritize locations of treated wastewater use considering climate change scenarios.
858 *JEM* 146, 505–516, <https://doi.org/10.1016/j.jenvman.2014.08.013>, 2014.
- 859 9. Cox, P., and Stephenson, D.: A changing climate for prediction. *Science* 317(5835),
860 207–208, <https://www.science.org/doi/10.1126/science.1145956>, 2007.
- 861 10. Deser, C., Phillips, A., Bourdette, V., and Teng, H.: Uncertainty in climate change
862 projections: the role of internal variability. *Clim. Dyn.* 38, 527–546,
863 <https://doi.org/10.1007/s00382-010-0977-x>, 2012
- 864 11. Déqué, M.: Frequency of precipitation and temperature extremes over France in an
865 anthropogenic scenario: Model results and statistical correction according to
866 observed values. *Glob. Planet. Change.* 57(1-2), 16-26,
867 <https://doi.org/10.1016/j.gloplacha.2006.11.030>, 2007.
- 868 12. Ehret, U., Zehe, E., Wulfmeyer, V., Warrach-Sagi, K., and Liebert, J.: HESS
869 Opinions "Should we apply bias correction to global and regional climate model

- 870 data?". HESS 16(9), 3391-3404, <https://doi.org/10.5194/hess-16-3391-2012>, 2012.
- 871 13. Enayati, M., Bozorg-Haddad, O., Bazrafshan, J., Hejabi, S., and Chu, X.: Bias
872 correction capabilities of quantile mapping methods for rainfall and temperature
873 variables. *Water and Climate change* 12(2), 401-419,
874 <https://doi.org/10.2166/wcc.2020.261>, 2021.
- 875 14. Evin, G., Ribes, A., and Corre, L.: Assessing CMIP6 uncertainties at global warming
876 levels. *Clim Dyn.* <https://doi.org/10.1007/s00382-024-07323-x>, 2024.
- 877 15. Eyring, V., Bony, S., Meehl, G., Senior, C., Stevens, B., Stouffer, R., and Taylor, K.:
878 **Overview of the Coupled Model Intercomparison Project Phase 6 (CMIP6)**
879 **experimental design and organization [Dataset]. *Geoscientific Model Development,***
880 **9(5), 1937–1958. 2016. <https://doi.org/10.5194/gmd-9-1937-2016>**
- 881 16. Galton, F.: Regression Towards Mediocrity in Hereditary Stature. *The Journal of the*
882 *Anthropological Institute of Great Britain and Ireland* 15, 246-263,
883 <https://doi.org/10.2307/2841583>, 1886.
- 884 17. Giorgi, F., and Mearns, L.O.: Calculation of average, uncertainty range, and
885 reliability of regional climate changes from AOGCM simulations via the “reliability
886 ensemble averaging” (REA) method, *J. Clim.* 15, 1141–1158,
887 [https://doi.org/10.1175/1520-0442\(2002\)015<1141:COAURA>2.0.CO;2](https://doi.org/10.1175/1520-0442(2002)015<1141:COAURA>2.0.CO;2), 2000.
- 888 18. Gupta, H.V., Kling, H., Yilmaz, K.K., and Martinez, G.F.: Decomposition of the
889 mean squared error and NSE performance criteria: Implications for improving
890 hydrological modelling. *J. Hydrol.* 377(1–2), 80–91,
891 <https://doi.org/10.1016/j.jhydrol.2009.08.003>, 2009
- 892 19. Gudmundsson, L., Bremnes, J.B., Haugen, J.E., and Engen-Skaugen, T.: Technical
893 Note: Downscaling RCM precipitation to the station scale using statistical
894 transformations – a comparison of methods. HESS 16(9), 3383–3390,
895 <https://doi.org/10.5194/hess-16-3383-2012>, 2012.
- 896 20. Hamed, M.M., Nashwan, M.S., Shahid, S., Wang, X.J., Ismail, T.B., Dewan, A., and
897 Asaduzzaman, M.d: Future Köppen-Geiger climate zones over Southeast Asia using
898 CMIP6 Multimodel Ensemble. *Atmos. Res.* 283(1), 106560,
899 <https://doi.org/10.1016/j.atmosres.2022.106560>, 2023.
- 900 21. Hersbach, H., Bell, B., Berrisford, P., Hirahara, S., Horányi, A., Muñoz-Sabater, J.,
901 Nicolas, J., Peubey, C., Radu, R., Schepers, D., Simmons, A., Soci, C., Abdalla, S.,

- 902 Abellan, X., Balsamo, G., Bechtold, P., Biavati, G., Bidlot, J., Bonavita, M., Chiara,
903 G., Dahlgren, P., Dee, D., Diamantakis, M., Dragani, R., Flemming, J., Forbes, R.,
904 Fuentes, M., Geer, A., Haimberger, L., Healy, S., Hogan, R. J., Hólm, E., Janisková,
905 M., Keeley, S., Laloyaux, P., Lopez, P., Lupu, C., Radnoti, G., Rosnay, P., Rozum,
906 I., Vamborg, F., Villaume, S., and Thépaut, J.: The ERA5 global reanalysis, *Q. J.*
907 *Roy. Meteor. Soc.*, 146, 1999–2049, <https://doi.org/10.1002/qj.3803>, 2020.
- 908 22. Hersbach, H., Bell, B., Berrisford, P., Biavati, G., Horányi, A., Muñoz Sabater, J.,
909 Nicolas, J., Peubey, C., Radu, R., Rozum, I., Schepers, D., Simmons, A., Soci, C.,
910 Dee, D., and Thépaut, J.-N.: ERA5 hourly data on pressure levels from 1940 to
911 present, Copernicus Climate Change Service (C3S) Climate Data Store (CDS) [Data
912 set], <https://doi.org/10.24381/cds.bd0915c6>, 2023.
- 913 23. Homsí, R., Shiru, M. S., Shahid, S., Ismail, T., Harun, S. B., Al-Ansari, N., and
914 Yaseen, Z.M: Precipitation projection using a CMIP5 GCM ensemble model: a
915 regional investigation of Syria. *Eng. Appl. Comput. Fluid Mech.* 14(1), 90–106,
916 <https://doi.org/10.1080/19942060.2019.1683076>, 2019.
- 917 24. Hoeting J.A., Madigan D., Raftery A.E., and Volinsky C.T.: Bayesian model
918 averaging: A tutorial (with discussion). *Stat. Sci.* 214, 382-417,
919 <https://doi.org/10.1214/ss/1009212519>, 1999.
- 920 25. Hosking, J.R.M., Wallis, J.R., and Wood, E.F.: Estimation of the generalized
921 extreme value distribution by the method of probability weighted moments.
922 *Technometrics* 27, 251–261, <https://doi.org/10.1080/00401706.1985.10488049>,
923 1985.
- 924 26. Hosking, J.R.M.: L-moments: Analysis and estimation of distributions using linear
925 combinations of order statistics. *J. R. Stat.* 52, 105–124,
926 <https://doi.org/10.1111/j.2517-6161.1990.tb01775.x>, 1990.
- 927 27. Hwang, C. L., and Yoon, K.: Multiple attribute decision making: Methods and
928 applications. Springer-Verlag. <https://doi.org/10.1007/978-3-642-48318-9>. 1981.
- 929 28. IPCC: Climate Change 2021: The Physical Science Basis. Contribution of Working
930 Group I to the Sixth Assessment Report of the Intergovernmental Panel on Climate
931 Change, edited by: Masson-Delmotte, V., Zhai, P., Pirani, A., Connors, S. L., Péan,
932 C., Berger, S., Caud, N., Chen, Y., Goldfarb, L., Gomis, M. I., Huang, M., Leitzell,
933 K., Lonnoy, E., Matthews, J. B. R., Maycock, T. K., Waterfield, T., Yelekçi, O., Yu,

- 934 R., and Zhou, B., Cambridge University Press,
935 <https://doi.org/10.1017/9781009157896>, 2021.
- 936 29. IPCC: Climate Change 2022: Impacts, Adaptation, and Vulnerability. Contribution
937 of Working Group II to the Sixth Assessment Report of the Intergovernmental Panel
938 on Climate Change, edited by: Pörtner, H.-O., Roberts, D. C., Tignor, M.,
939 Poloczanska, E. S., Mintenbeck, K., Alegría, A., Craig, M., Langsdorf, S., Lösschke,
940 S., Möller, V., Okem, A., and Rama, B., Cambridge University Press,
941 <https://doi.org/10.1017/9781009325844>, 2022.
- 942 30. Ishizaki, N.N., Shiogama, H., Hanasaki, N., Takahashi, K., and Nakaegawa, T.:
943 Evaluation of the spatial characteristics of climate scenarios based on statistical and
944 dynamical downscaling for impact assessments in Japan. *Int. J. Climatol.* 43(2),
945 1179-1192, <https://doi.org/10.1002/joc.7903>, 2022.
- 946 31. Jobst, A.M., Kingston, D.G., Cullen, N.J., and Schmid, J.: Intercomparison of
947 different uncertainty sources in hydrological climate change projections for an alpine
948 catchment (upper Clutha River, New Zealand). *HESS* 22, 3125-3142,
949 <https://doi.org/10.5194/hess-22-3125-2018>, 2018.
- 950 32. Lafferty, D.C., and Sriver, R.L.: Downscaling and bias-correction contribute
951 considerable uncertainty to local climate projections in CMIP6. *npj Clim Atmos*
952 *Sci* 6, 158, <https://doi.org/10.1038/s41612-023-00486-0>, 2023.
- 953 33. Lafon, T., Dadson, S., Buys, G., and Prudhomme, C.: Bias correction of daily
954 precipitation simulated by a regional climate model: a comparison of methods. *Int. J.*
955 *Climatol.* 33, 1367-1381, <http://dx.doi.org/10.1002/joc.3518>, 2013.
- 956 34. Lin, J.: Divergence measures based on the Shannon entropy. *IEEE Transactions on*
957 *Information Theory* 37(1), 145–151, <https://doi.org/10.1109/18.61115>, 1991.
- 958 35. Maraun, D.: Bias correction, quantile mapping, and downscaling: Revisiting the
959 inflation issue. *J. Clim.* 26(6), 2137-2143, [https://doi.org/10.1175/JCLI-D-12-](https://doi.org/10.1175/JCLI-D-12-00821.1)
960 [00821.1](https://doi.org/10.1175/JCLI-D-12-00821.1), 2013.
- 961 36. Nair, M.M.A., Rajesh, N., Sahai, A.K., and Lakshmi Kumar, T.V.: Quantification of
962 uncertainties in projections of extreme daily precipitation simulated by CMIP6
963 GCMs over homogeneous regions of India. *Int. J. Climatol.* 43(15), 7365-7380,
964 <https://doi.org/10.1002/joc.8269>, 2023.
- 965 37. Nash, J.E., and Sutcliffe, J.V.: River flow forecasting through conceptual models part

- 966 I—A discussion of principles. *J. Hydrol.* 10, 282–290, <https://doi.org/10.1016/0022->
967 1694(70)90255-6Return to ref 1970 in article, 1970.
- 968 38. Pathak, R., Dasari, H.P., Ashok, K., and Hoteit, I., Effects of multi-observations
969 uncertainty and models similarity on climate change projections. *npj clim. atmos. sci.*
970 6, 144, <https://doi.org/10.1038/s41612-023-00473-5>, 2023.
- 971 39. Piani, C., Weedon, G. P., Best, M., Gomes, S. M., Viterbo, P., Hagemann, S., and
972 Haerter, J.O.: Statistical bias correction of global simulated daily precipitation and
973 temperature for the application of hydrological models. *J. Hydrol.* 395(3-4), 199-215,
974 <https://doi.org/10.1016/j.jhydrol.2010.10.024>, 2010.
- 975 40. Rahimi, R., Tavakol-Davani, H., and Nasser, M.: An Uncertainty-Based Regional
976 Comparative Analysis on the Performance of Different Bias Correction Methods in
977 Statistical Downscaling of Precipitation. *Water Resour. Manag.* 35, 2503–2518,
978 <https://doi.org/10.1007/s11269-021-02844-0>, 2021.
- 979 41. Rajulapati, C.R., and Papalexiou, S.M.: Precipitation Bias Correction: A Novel
980 Semi-parametric Quantile Mapping Method. *Earth Space Sci.* 10(4),
981 e2023EA002823, <https://doi.org/10.1029/2023EA002823>, 2023.
- 982 42. Saranya, M.S., and Vinish, V.N.: Evaluation and selection of CORDEX-SA datasets
983 and bias correction methods for a hydrological impact study in a humid tropical river
984 basin, Kerala. *Water Climate Change* 12(8), 3688-3713,
985 <https://doi.org/10.2166/wcc.2021.139>, 2021.
- 986 43. Shanmugam, M., Lim, S., Hosan, M.L. Shrestha, S., Babel, M.S., and Viridis, S.G.P.:
987 Lapse rate-adjusted bias correction for CMIP6 GCM precipitation data: An
988 application to the Monsoon Asia Region. *Environ Monit Assess.* 196, 49,
989 <https://doi.org/10.1007/s10661-023-12187-5>, 2024.
- 990 44. Song, J. Y., and Chung, E.S.: Robustness, uncertainty, and sensitivity analyses of
991 TOPSIS method to climate change vulnerability: Case of flood damage. *Water*
992 *Resour. Manag.*, 30(13), 4751–4771, <https://doi.org/10.1007/s11269-016-1451-2>,
993 2016.
- 994 45. Song, Y.H., Shahid, S., and Chung, E.S.: Differences in multi-model ensembles of
995 CMIP5 and CMIP6 projections for future droughts in South Korea. *Int. J. Climatol.*
996 42(5), 2688-2716, <https://doi.org/10.1002/joc.7386>, 2022a.
- 997 46. Song, Y.H., Chung, E.S., and Shahid, S.: The New Bias Correction Method for Daily

- 998 Extremes Precipitation over South Korea using CMIP6 GCMs. *Water Resour.*
999 *Manag.* 36, 5977–5997, <https://doi.org/10.1007/s11269-022-03338-3>, 2022b.
- 1000 47. Song, Y.H., Chung, E.S., and Shahid, S.: Uncertainties in evapotranspiration
1001 projections associated with estimation methods and CMIP6 GCMs for South Korea.
1002 *Sci. Total Environ.* 825, 153953, <https://doi.org/10.1016/j.scitotenv.2022.153953>,
1003 2023.
- 1004 48. Song, Y.H., Chung, E.S., and Shahid, S.: Global Future Climate Signal by Latitudes
1005 Using CMIP6 GCMs. *Earths Future* 12(3), e2022EF003183,
1006 <https://doi.org/10.1029/2022EF003183>, 2024.
- 1007 49. Song, Y.H.: **Comprehensive Index and Performance-Related Code, Figshare [Code],**
1008 <https://doi.org/10.6084/m9.figshare.27987665.v2>
- 1009 50. Switanek, M.B., Troch, P.A., Castro, C.L., Leuprecht, A., Chang, H.I., Mukherjee,
1010 R., and Demaria E.M.C.: Scaled distribution mapping: a bias correction method that
1011 preserves raw climate model projected changes. *HESS* 21(6), 2649-2666,
1012 <https://doi.org/10.5194/hess-21-2649-2017>, 2017.
- 1013 51. Tanimu, B., Bello, A.A.D., Abdullahi, S.A. Ajibike, M.A., Yaseen, Z.M.,
1014 Kamruzzaman, M., Muhammad, M.K.I., and Shahid, S.: Comparison of conventional
1015 and machine learning methods for bias correcting CMIP6 rainfall and temperature in
1016 Nigeria. *Theor. Appl. Climatol.* 155, 4423–4452, [https://doi.org/10.1007/s00704-](https://doi.org/10.1007/s00704-024-04888-9)
1017 [024-04888-9](https://doi.org/10.1007/s00704-024-04888-9), 2024.
- 1018 52. Teutschbein, C., AND Seibert, J.: Bias correction of regional climate model
1019 simulations for 575 hydrological climate-change impact studies: Review and
1020 evaluation of different 576 methods. *J. Hydrol.* 16, 12-29,
1021 <http://dx.doi.org/10.1016/j.jhydrol.2012.05.052>, 2012.
- 1022 53. Teng, J., Potter, N. J., Chiew, F. H. S., Zhang, L., Wang, B., Vaze, J., and Evans,
1023 J.P.: 2015. How does bias correction of regional climate model precipitation affect
1024 modelled runoff? *HESS* 19, 711–728, <https://doi.org/10.5194/hess-19-711-2015>,
1025 2015.
- 1026 54. Themeßl, M.J., Gobiet, A., and Heinrich, G.: Empirical-statistical downscaling and
1027 error correction of daily precipitation from regional climate models. *Int. J. Climatol.*
1028 31(10), 1530-1544, <https://doi.org/10.1002/joc.2168>, 2012.
- 1029 55. Tong, Y., Gao, X., Han, Z., Xu, Y., and Giorgi, F.: Bias correction of temperature

- 1030 and precipitation over China for RCM simulations using the QM and QDM methods.
1031 *Clim. Dyn.* 57, 1425-1443, <https://doi.org/10.1007/s00382-020-05447-4>, 2021.
- 1032 56. Yip, S., Ferro, C.A.T., Stephenson, D.B., and Hawkins, E.: A simple, coherent
1033 framework for partitioning uncertainty in climate predictions. *J. Clim.* 24(17), 4634–
1034 4643, <https://doi.org/10.1175/2011JCLI4085.1>, 2011.
- 1035 57. Woldemeskel, F. M., Sharma, A. Sivakumar, B., and Mehrotra, R.: A framework to
1036 quantify GCM uncertainties for use in impact assessment studies. *J. Clim.* 519,
1037 1453–1465, <https://doi.org/10.1016/j.jhydrol.2014.09.025>, 2014.
- 1038 58. Wu, Y., Miao, C., Fan, X., Gou, J., Zhang, Q., and Zheng, H.: Quantifying the
1039 uncertainty sources of future climate projections and narrowing uncertainties with
1040 Bias Correction Techniques. *Earths Future*, 10(11), e2022EF002963, 2022.
- 1041 59. Zhang, S., Zhou, Z., Peng, P., and Xu, C.: A New Framework for Estimating and
1042 Decomposing the Uncertainty of Climate Projections. *J. Clim.* 37(2), 365-384,
1043 <https://doi.org/10.1175/JCLI-D-23-0064.1>, 2024.
- 1044